References

1. Chen SH, Chen XH, Wang Y, Kosai K, Finegold MJ, Rich SS and Woo SL: Combination gene therapy for liver metastasis of colon carcinoma *in vivo*. Proc Natl Acad Sci USA 92: 2577-2581, 1995.
2. Huang H, Chen SH, Kosai K, Finegold MJ, and Woo SL: Gene therapy for hepatocellular carcinoma: long-term remission of primary and metastatic tumors in mice by interleukin-2 gene therapy *in vivo*. Gene Ther 3: 980-987, 1996.
3. Caruso M, Pham-Nguyen K, Kwong YL, *et al*: Adenovirus-mediated interleukin-12 gene therapy for metastatic colon carcinoma. Proc Natl Acad Sci USA 93: 11302-11306, 1996.
4. O'Malley BW Jr, Sewell DA, Li D, Kosai K, Chen SH, Woo SL and Duan L: The role of interleukin-2 in combination adenovirus gene therapy for head and neck cancer. Mol Endocrinol 11: 667-673, 1997.
5. Kwong YL, Chen SH, Kosai K, Finegold M and Woo SL: Combination therapy with suicide and cytokine genes for hepatic metastases of lung cancer. Chest 112: 1332-1337, 1997.
6. Moller GT: T cell stimulating growth factors. Immunol Rev 51: 1-357, 1980.
7. Fearon ER, Pardoll DM, Itaya T, *et al*: Interleukin-2 production by tumor cells bypasses T helper function in the generation of an antitumor response. Cell 60: 397-403, 1990.
8. Henney CS, Kuribayashi K, Kern DE and Gillis S: Interleukin-2 augments natural killer cell activity. Nature 291: 335-338, 1981.
9. Lotze MT, Grimm EA, Mazumder A, Strausser JL and Rosenberg SA: Lysis of fresh and cultured autologous tumor by human lymphocytes cultured in T-cell growth factor. Cancer Res 41: 4420-4425, 1981.
10. Trinchieri G: Biology of natural killer cells. Adv Immunol 47: 187-376, 1989.
11. Smith KA: Interleukin-2: inception, impact, and implications. Science 240: 1169-1176, 1988.
12. Parmiani G, Rivoltini L, Andreola G and Carrabba M: Cytokines in cancer therapy. Immunol Lett 74: 41-44, 2000.
13. Marshall E: Cancer therapy. Setbacks for endostatin. Science 295: 2198-2199, 2002.
14. Galanis E and Russell S: Cancer gene therapy clinical trials: lessons for the future. Br J Cancer 85: 1432-1436, 2001.
15. McCormick F: Cancer gene therapy: fringe or cutting edge? Nat Rev Cancer 1: 130-141, 2001.
16. Kiwaki K, Kanegae Y, Saito I, *et al*: Correction of ornithine transcarbamylase deficiency in adult spf(ash) mice and in OTC-deficient human hepatocytes with recombinant adenoviruses bearing the CAG promoter. Hum Gene Ther 7: 821-830, 1996.
17. Ye X, Robinson MB, Batshaw ML, Furth EE, Smith I and Wilson JM: Prolonged metabolic correction in adult ornithine transcarbamylase-deficient mice with adenoviral vectors. J Biol Chem 271: 3639-3646, 1996.
18. Lehrman S: Virus treatment questioned after gene therapy death. Nature 401: 517-518, 1999.
19. Fukunaga M, Takamori S, Hayashi A, Shirouzu K and Kosai K: Adenoviral herpes simplex virus thymidine kinase gene therapy in an orthotopic lung cancer model. Ann Thorac Surg 73: 1740-1746, 2002.
20. Terazaki Y, Yano S, Yuge K, *et al*: An optimal therapeutic expression level is crucial for suicide gene therapy for hepatic metastatic cancer in mice. Hepatology 37: 155-163, 2003.
21. Papagelopoulos PJ, Galanis EC, Vlastou C, *et al*: Current concepts in the evaluation and treatment of osteosarcoma. Orthopedics 23: 858-867, 2000.
22. Dome JS and Schwartz CL: Osteosarcoma. Cancer Treat Res 92: 215-251, 1997.
23. Saeter G, Hoie J, Stenwig AE, Johansson AK, Hannisdal E and Solheim OP: Systemic relapse of patients with osteogenic sarcoma. Prognostic factors for long term survival. Cancer 75: 1084-1093, 1995.
24. Bacci G, Briccoli A, Ferrari S, *et al*: Neoadjuvant chemotherapy for osteosarcoma of the extremity: long-term results of the Rizzoli's 4th protocol. Eur J Cancer 37: 2030-2039, 2001.
25. Marina NM, Pratt CB, Rao BN, Shema SJ and Meyer WH: Improved prognosis of children with osteosarcoma metastatic to the lung(s) at the time of diagnosis. Cancer 70: 2722-2727, 1992.
26. Bacci G, Briccoli A, Ferrari S, *et al*: Neoadjuvant chemotherapy for osteosarcoma of the extremities with synchronous lung metastases: treatment with cisplatin, adriamycin and high dose of methotrexate and ifosfamide. Oncol Rep 7: 339-346, 2000.
27. Asai T, Ueda T, Itoh K, Yoshioka K, Aoki Y, Mori S and Yoshikawa H: Establishment and characterization of a murine osteosarcoma cell line (LM8) with high metastatic potential to the lung. Int J Cancer 76: 418-422, 1998.
28. Ko SC, Gotoh A, Thalmann GN, *et al*: Molecular therapy with recombinant p53 adenovirus in an androgen-independent, metastatic human prostate cancer model. Hum Gene Ther 7: 1683-1691, 1996.
29. Greenberg DB, Goorin A, Gebhardt MC, Gupta L, Stier N, Harmon D and Mankin H: Quality of life in osteosarcoma survivors. Oncology 8: 19-35, 1994.
30. Lane JM, Christ GH, Khan SN and Backus SI: Rehabilitation for limb salvage patients: kinesiological parameters and psychological assessment. Cancer 92: 1013-1019, 2001.
31. Pandha HS, Martin LA, Rigg AS, Ross P and Dalgleish AG: Gene therapy: recent progress in the clinical oncology arena. Curr Opin Mol Ther 2: 362-375, 2000.
32. Smith AE: Gene therapy - where are we? Lancet 354 (Suppl. 1): SI1-S4, 1999.
33. Okada Y, Okada N, Nakagawa S, *et al*: Fiber-mutant technique can augment gene transduction efficacy and anti-tumor effects against established murine melanoma by cytokine-gene therapy using adenovirus vectors. Cancer Lett 177: 57-63, 2002.
34. Gomez-Navarro J, Curiel DT and Douglas JT: Gene therapy for cancer. Eur J Cancer 35: 2039-2057, 1999.
35. Bonnekoh B, Greenhalgh DA, Bundman DS, *et al*: Adenoviral-mediated herpes simplex virus-thymidine kinase gene transfer *in vivo* for treatment of experimental human melanoma. J Invest Dermatol 106: 1163-1168, 1996.
36. Kwong YL, Chen SH, Kosai K, Finegold MJ and Woo SL: Adenoviral-mediated suicide gene therapy for hepatic metastases of breast cancer. Cancer Gene Ther 3: 339-344, 1996.
37. Block A, Chen SH, Kosai K, Finegold M and Woo SL: Adenoviral-mediated herpes simplex virus thymidine kinase gene transfer: regression of hepatic metastasis of pancreatic tumors. Pancreas 15: 25-34, 1997.

Oncogene (2004), 1–9

www.nature.com/onc

ORIGINAL PAPER

Tumor suppressor WARTS ensures genomic integrity by regulating both mitotic progression and G_1 tetraploidy checkpoint function

Shin-ichi Iida[1,2], Toru Hirota[1], Tetsuro Morisaki[1], Tomotoshi Marumoto[1], Toshihiro Hara[1], Shinji Kuninaka[1], Shinobu Honda[1], Ken-ichiro Kosai[3], Michio Kawasuji[2], David C Pallas[4] and Hideyuki Saya*[,1]

[1]Department of Tumor Genetics and Biology, Graduate School of Medical Sciences, Kumamoto University, 1-1-1 Honjo, Kumamoto 860-8556, Japan; [2]Department of Cardiovascular Surgery, Graduate School of Medical Sciences, Kumamoto University, 1-1-1 Honjo, Kumamoto 860-8556, Japan; [3]Division of Gene Therapy and Regenerative Medicine, Cognitive and Molecular Research Institute of Brain Diseases Kurume University, Kurume 830-0011, Japan; [4]Department of Biochemistry and Winship Cancer Center, Emory University School of Medicine, Atlanta, GA 30322, USA

Defects in chromosomes or mitotic spindles activate the spindle checkpoint, resulting in cell cycle arrest at prometaphase. The prolonged activation of spindle checkpoint generally leads to mitotic exit without segregation after a transient mitotic arrest and the consequent formation of tetraploid G_1 cells. These tetraploid cells are usually blocked to enter the subsequent S phase by the activation of p53/pRb pathway, which is referred to as the G_1 tetraploidy checkpoint. A human homologue of the *Drosophila* warts tumor suppressor, WARTS, is an evolutionarily conserved serine–threonine kinase and implicated in development of human tumors. We previously showed that WARTS plays a crucial role in controlling mitotic progression by forming a regulatory complex with zyxin, a regulator of actin filament assembly, on mitotic apparatus. However, when WARTS is activated during cell cycle and how the loss of WARTS function leads to tumorigenesis have not been elucidated. Here we show that WARTS is activated during mitosis in mammalian cells, and that overexpression of a kinase-inactive WARTS in Rat1 fibroblasts significantly induced mitotic delay. This delay resulted from prolonged activation of the spindle assembly checkpoint and was frequently followed by mitotic slippage and the development of tetraploidy. The resulting tetraploid cells then abrogated the G_1 tetraploidy checkpoint and entered S phase to achieve a DNA content of 8N. This impairment of G_1 tetraploidy checkpoint was caused as a consequence of failure to induce p53 expression by expressing a kinase-inactive WARTS. WARTS thus plays a critical role in maintenance of ploidy through its actions in both mitotic progression and the G_1 tetraploidy checkpoint.
Oncogene advance online publication, 3 May 2004; doi:10.1038/sj.onc.1207623

Keywords: cell cycle; mitotic kinase; spindle checkpoint; p53; polyploid

*Correspondence: H Saya; E-mail: hsaya@gpo.kumamoto-u.ac.jp
Received 4 December 2003; revised 10 February 2004; accepted 12 February 2004

Introduction

Mitosis is precisely regulated by sequential biochemical reactions, including protein phosphorylation and degradation, in order to achieve the equal separation of replicated sister chromatids into the two daughter cells. Checkpoints exist at various stages of the cell cycle to prevent improper progression of cells through the cycle and thereby to preserve the integrity of the genome. During mitotic phase, the spindle assembly checkpoint plays an important role in ensuring that chromosomes align correctly at the metaphase plate in preparation for their segregation. Defects in chromosomes or the mitotic spindle at this stage result in activation of the spindle assembly checkpoint and cell cycle arrest at prometaphase. Prolonged activation of this checkpoint leads to the skipping of chromosome segregation and cytokinesis and the consequent formation of tetraploid cells. The replication of DNA in tetraploid cells that have entered the subsequent G_1 phase is usually blocked by p53- and pRb-dependent cell cycle arrest, which is referred to as the G_1 tetraploidy checkpoint (Margolis *et al.*, 2003). Impairment of this checkpoint allows the tetraploid cells to maintain their proliferative potential, a process known as tetraploidization. Mitotic dysfunction alone is thus not sufficient to induce and maintain tetraploidization, which is considered a frequent precursor of aneuploidy during tumorigenesis (Shackney *et al.*, 1989).

The *warts* gene (also referred to as *lats*) was identified on the basis of its ability to act as a tumor suppressor in *Drosophila melanogaster* (Justice *et al.*, 1995). The protein encoded by this gene possesses a serine–threonine kinase catalytic domain that is highly similar to those of members of the human myotonic dystrophy protein kinase family. Kinases of this family have been shown to contribute to various mitotic events (Toyn and Johnston, 1994; Yasui *et al.*, 1998). A human homolog of warts, termed WARTS (or LATS1), has been identified (Nishiyama *et al.*, 1999; Tao *et al.*, 1999), and mice deficient in the corresponding protein develop malignant tumors similarly to the analogous *Drosophila* mutant (St John *et al.*, 1999). Furthermore, a missense

point mutation of *WARTS* was recently identified in human soft-tissue sarcoma, suggesting that alterations in WARTS function might be of pathological importance in human tumorigenesis (Hisaoka *et al*., 2002).

Immunolocalization studies have shown that human WARTS is found in cytoplasm and the centrosome in interphase cells, that it localizes to the mitotic apparatus, including the spindle poles and mitotic spindle, during metaphase–anaphase, and that it is present at the midbody during telophase (Nishiyama *et al*., 1999). Moreover, WARTS is phosphorylated during mitosis and interacts with zyxin, a regulator of actin filament assembly, at the mitotic apparatus, and this mitosis-specific interaction plays an important role in the control of mitotic progression (Hirota *et al*., 2000). WARTS is thus a key player in mitotic events in mammalian cells, and loss of its function disrupts normal mitotic regulation, possibly leading to chromosomal instability and tumor development. However, given that the kinase activity of WARTS in cells has not been unambiguously detected to date, the mechanisms by which WARTS contributes to cell cycle events have remained largely unknown.

To provide insight into WARTS function, we have now examined the kinase activity of this protein during the cell cycle in mammalian cells. WARTS was activated specifically during mitosis, with peak activity apparent at the prometaphase/metaphase transition. Overexpression of a kinase-inactive WARTS mutant in Rat1 fibroblasts induced a pronounced delay in entry into anaphase as well as subsequent mitotic slippage and the development of tetraploidy. Furthermore, such tetraploid cells did not arrest at G_1 phase and entered another round of DNA synthesis, resulting in tetraploidization. In contrast, Rat1 cells overexpressing wild-type WARTS underwent cell death when the spindle assembly checkpoint was continuously activated by nocodazole treatment. Our results suggest that the kinase activity of WARTS is required for proper mitotic progression, for cell death in response to prolonged activation of the spindle assembly checkpoint, and for activation of the G_1 tetraploidy checkpoint. The loss of WARTS function might thus induce mitotic aberration followed by tetraploidization, which leads to the consequent development of aneuploidy during tumorigenesis.

Results

Mitotic activation of WARTS kinase activity

To investigate possible changes in the kinase activity of human WARTS during the cell cycle, we first performed *in vitro* kinase assays with WARTS immunoprecipitated from asynchronous or mitotic HeLa cells. Whereas, autophosphorylation of WARTS *in vitro* was almost undetectable with the protein isolated from asynchronous cells, it was markedly increased with WARTS derived from mitotic cells (Figure 1a). To exclude the possibility that phosphorylation of WARTS detected in this assay was due to the presence of another kinase in the immunoprecipitates, we generated stable transfectants of Rat1 fibroblasts that constitutively express wild-type or kinase-inactive forms of WARTS tagged at their NH_2-termini with the Myc epitope (WTW1 and KDW1 cells, respectively) (Figure 1b). The kinase-inactive WARTS mutant (K734A) was constructed by replacing lysine 734 with alanine. This conserved lysine residue has been proven to play a key role in the recognition of the phosphate group of Mg-ATP (Hanks *et al*., 1988), and changing this lysine residue reportedly resulted in a kinase-inactive protein (Xia *et al*., 2002). Both exogenous WARTS proteins localized to centrosomes and the cytoplasm during interphase and to the mitotic apparatus during mitosis (Figure 1c), consistent with the cell cycle-dependent localization of the endogenous protein as previously reported (Nishiyama *et al*., 1999).

To examine whether the kinase activity of wild-type Myc-WARTS was increased during mitosis like that of endogenous WARTS, we synchronized WTW1 cells at prometaphase by treatment with nocodazole and then released them into normal medium. Myc-WARTS was immunoprecipitated from cell lysates at various times thereafter with antibodies to Myc and was subjected to the *in vitro* kinase assay. A protein that migrated at the position of Myc-WARTS was phosphorylated during mitotic progression, with the maximal activity apparent 10–15 min after release from prometaphase arrest (Figure 1d). However, no phosphorylated protein of the same size was detected when the same experiment was performed with KDW1 cells (Figure 1e). Furthermore, Myc-WARTS immunoprecipitated from asynchronous WTW1 cells exhibited only a low level of autophosphorylation activity (Figure 1e). These findings indicated that WARTS is autophosphorylated, rather than phosphorylated by other kinases interacting with WARTS, during mitosis and that WARTS is thus activated specifically during M phase.

Chromosomal instability induced by overexpression of kinase-inactive WARTS

We next investigated the effects of constitutive expression of the wild-type and mutant WARTS proteins on the phenotype of Rat1 cells. The rate of proliferation was reduced in WTW1 cells and, to an even greater extent, in KDW1 cells compared with that apparent in parental Rat1 cells (Figure 2a). Flow cytometric analysis of WTW1 cells revealed two prominent peaks of cells in G_1 (2N) and in G_2–M (4N), similar to the cell cycle distribution of the parental cells (Figure 2b). In contrast, the proportion of 2N cells was reduced and that of 4N and >4N cells was increased for KDW1 cells compared with parental cells. These observations were supported by microscopic analysis of cells stained with propidium iodide to reveal DNA; nuclei of KDW1 cells thus tended to be much larger than those of WTW1 and parental Rat1 cells (Figure 2c). In addition, KDW1 cells frequently manifested lagging chromosomes during mitosis as well as enlarged, multilobular, or multiple nuclei (data not shown).

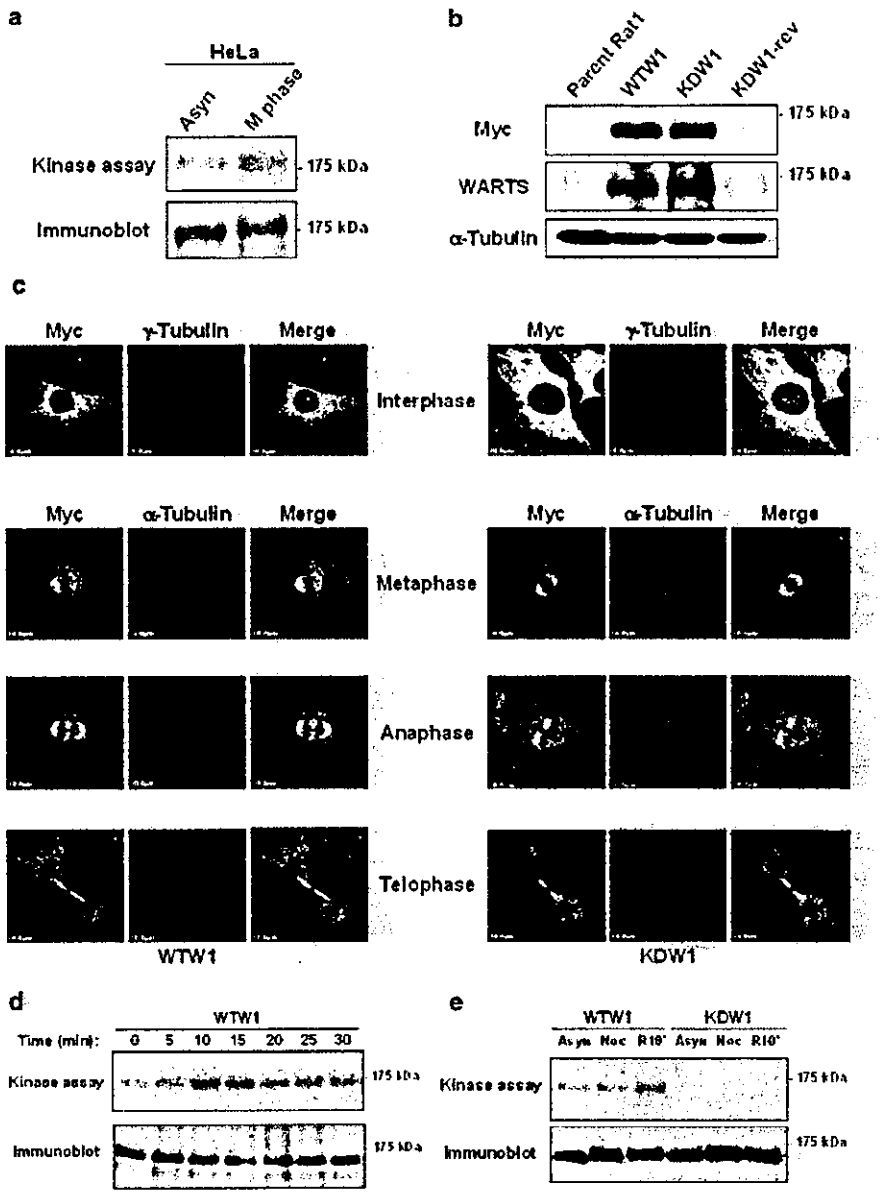

Figure 1 Mitosis-specific activation of WARTS. (a) Autophosphorylation of WARTS kinase during mitosis. Asynchronous (Asyn) or mitotic HeLa cells were lysed and subjected to immunoprecipitation with antibodies to WARTS, and the resulting precipitates were subjected either to immunoblot analysis with the same antibodies (bottom panel) or to an *in vitro* kinase assay with [γ-^{32}P]ATP (top panel). (b) Immunoblot analysis of Myc-WARTS expression. Total lysates of parental Rat1, WTW1, KDW1, and KDW1-rev cells were subjected to SDS–PAGE on a 6% gel followed by immunoblot analysis with antibodies to Myc (9E10), to WARTS (Hirota *et al*., 2000), or to α-tubulin (B-5-1-2) as a loading control. (c) Subcellular localization of Myc-WARTS during the cell cycle. WTW1 and KDW1 cells were fixed and processed for indirect immunofluorescence staining. Cells at interphase were immunostained with antibodies to Myc (FITC, green) and to γ-tubulin (Alexa 568, red); cells at metaphase, anaphase, or telophase were immunostained with antibodies to Myc (FITC, green) and to α-tubulin (Alexa 568, red). (d) Activation of wild-type Myc-WARTS during mitosis. WTW1 cells were treated with nocodazole for 10 h and then released into normal medium for the indicated times. Cell lysates were then subjected to immunoprecipitation with antibodies to Myc, and the resulting precipitates were subjected to the *in vitro* kinase assay with [γ-^{32}P]ATP. The same amounts of immunoprecipitates were then subjected to immunoblot analysis with antibodies to WARTS. (e) WTW1 or KDW1 cells were treated with nocodazole for 10 h and then released into normal medium for 0 (Noc) or 10 (R10′) min before analysis as in (d). Asynchronous cells were similarly analysed

To confirm the increased ploidy of KDW1 cells, we counted the chromosomes of the three cell types. The distribution of chromosome number for KDW1 cells differed markedly from that for WTW1 or parental Rat1 cell populations (Figure 2d). Of 50 metaphase KDW1 cells scored, 15 cells (30%) appeared almost tetraploid, whereas all parental Rat1 cells or WTW1 cells scored were diploid. The fact that intermediate

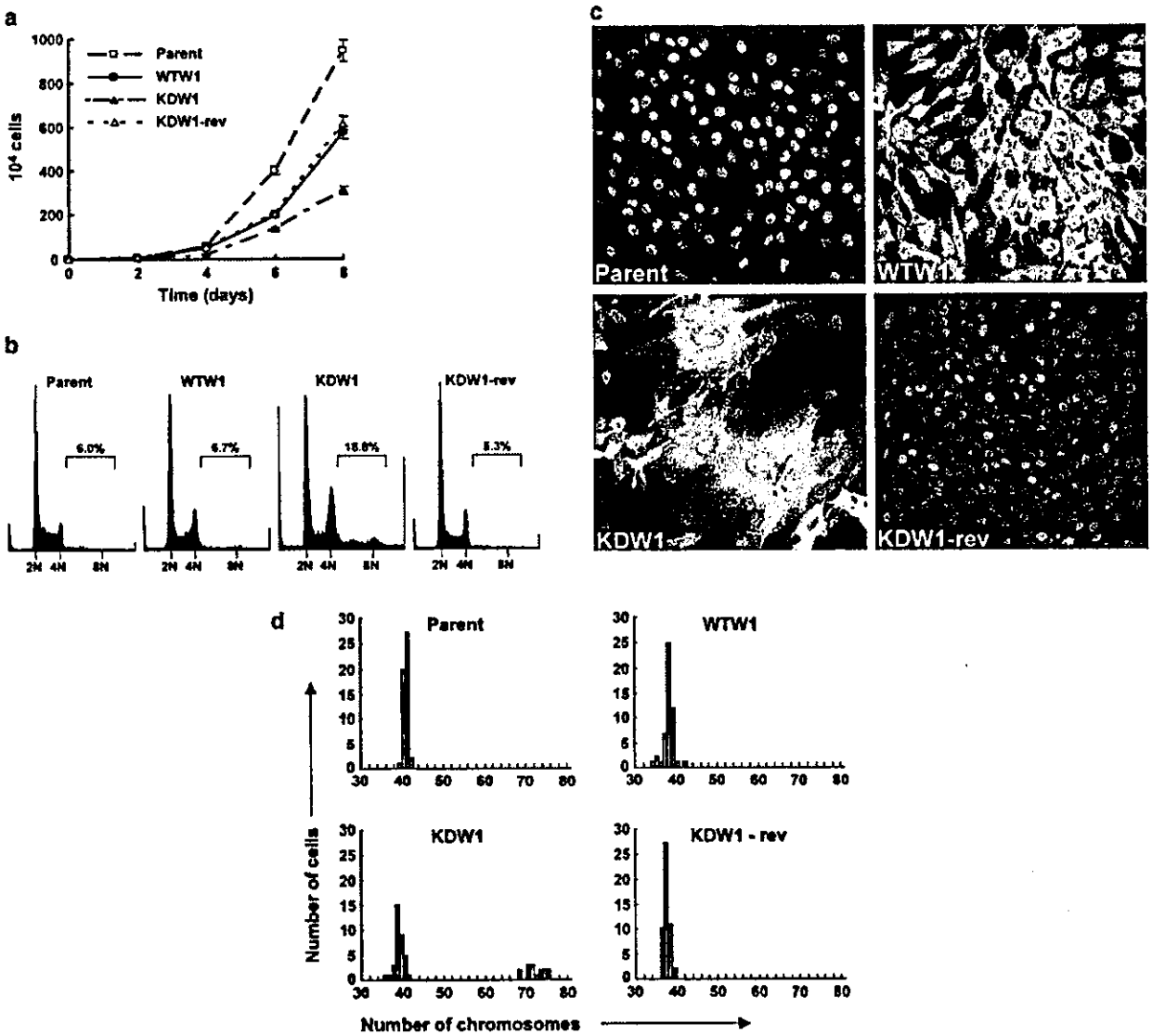

Figure 2 Polyploidy in Rat1 cells induced by overexpression of kinase-inactive WARTS. (a) Cell proliferation was analysed by seeding 1×10^4 cells (parental Rat1, WTW1, KDW1, or KDW1-rev) in complete medium into 10-cm dishes and determining the cell number every 48 h. Data are means$\pm$s.e.m. of values from three independent experiments. (b) Flow cytometric analysis of asynchronous cell cultures. Cells were harvested with trypsin-EDTA, fixed with 70% ethanol, treated with RNase A (100 U/ml), and stained with propidium iodide (50 μg/ml). Percentages represent the number of cells with a DNA content of >4N. (c) Nuclear morphology of parental Rat1, WTW1, KDW1, and KDW1-rev cells. Cells were fixed and processed for indirect immunofluorescence staining with antibodies to Myc (FITC, green) and for staining of DNA with propidium iodide (red). (d) Distribution of chromosome number was determined for 50 metaphase cells of the four cell lines

levels of ploidy were not observed in KDW1 cells suggested that the tetraploidy of these cells might result from either failure of chromosome segregation or impairment of cytokinesis.

At later passages (>23 doublings), KDW1 cells are somewhat unstable, generally containing some cells (~10% of the total population) that have lost the expression of the kinase-inactive form of WARTS protein (Figures 1b and 2c). We cloned these revertant KDW1 cells (termed KDW1-rev cells) and showed that they were phenotypically similar to WTW1 or parental Rat1 cells (Figure 2). The expression of the kinase-inactive WARTS protein thus appeared to be directly associated with the polyploid phenotype of KDW1 cells, suggesting that the kinase activity of WARTS is required for maintenance of ploidy.

Prolonged activation of the spindle assembly checkpoint induced by overexpression of kinase-inactive WARTS

To define more precisely the effect of the kinase-inactive WARTS on mitotic progression, we determined the

duration of mitosis in parental Rat1, WTW1, KDW1, and KDW1-rev cells with the use of time-lapse differential interference contrast microscopy. More than 90% of parental Rat1 or WTW1 cells executed mitosis within 30 min, whereas only 4% of KDW1 cells exited mitosis within this time (Figure 3a). In KDW1-rev cells, lost of the kinase-inactive WARTS expression significantly increased the number of cells (54%) exiting mitosis within 30 min. Most KDW1 cells with a prolonged duration of mitosis (>100 min) exited mitosis without undergoing cytokinesis. Expression of the kinase-inactive WARTS mutant thus interfered with normal mitotic progression and frequently induced skipping mitosis followed by polyploidization. These phenotypes might contribute to the reduced growth rate of KDW1 cells in comparison to WTW1 or KDW1-rev cells (Figure 2a).

To examine the nature of the mitotic delay in cells expressing the WARTS mutant, we synchronized WTW1 and KDW1 cells at prometaphase by nocodazole treatment, released them into normal medium, and then determined their mitotic distribution at various times thereafter by immunostaining with antibodies to α-tubulin and staining of DNA with propidium iodide. Whereas WTW1 cells began to enter anaphase after 15 min and had reached telophase by 25 min after release, most KDW1 cells remained in metaphase 25 min after release (Figure 3b). Quantitative analysis confirmed that KDW1 cells manifested a marked delay in anaphase entry compared with WTW1 cells (Figure 3c).

Delay in anaphase entry is usually caused either by activation of the spindle assembly checkpoint or by disruption of proteolysis by the anaphase-promoting complex or cyclosome (APC/C) (King *et al.*, 1995; Tugendreich *et al.*, 1995; Amon, 1999). To investigate the former possibility, we examined recruitment of MAD2 protein to kinetochores, which is thought to occur specifically at unattached kinetochores during prometaphase and is required for maintenance of spindle assembly checkpoint signaling (Shah and

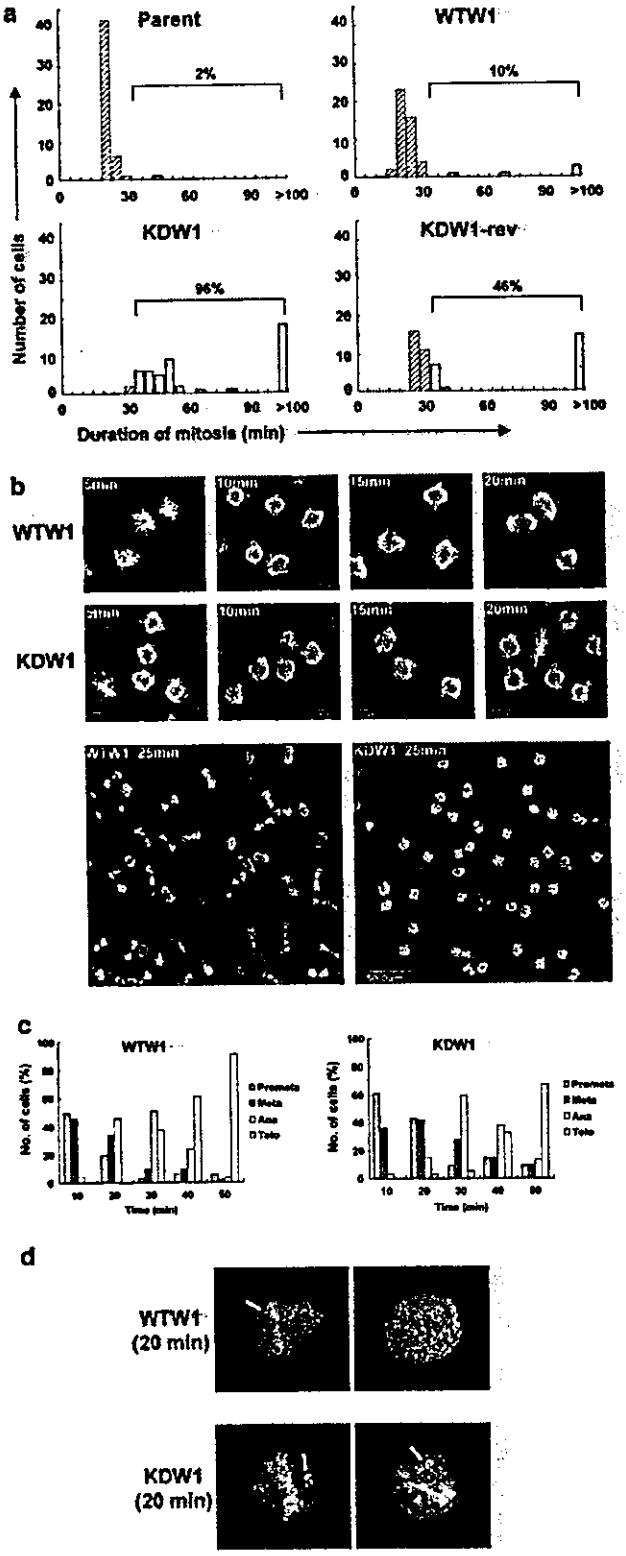

Figure 3 Mitotic delay due to activation of the spindle assembly checkpoint in cells overexpressing kinase-inactive WARTS. (**a**) Quantitation of the time required for individual parental Rat1, WTW1, KDW1, and KDW1-rev cells to complete mitosis. The duration of mitosis was determined morphologically by time-lapse videomicroscopy; its onset was defined as the time when the cell first became rounded and refractile and its end was defined as the time when the cell flattened back onto the dish. A total of 50 cells were analysed for each cell line. Percentages represent the number of cells that required >30 min to execute mitosis. (**b**) Characterization of mitotic progression in WTW1 and KDW1 cells. Cells were treated with nocodazole for 10 h and then released into normal medium for the indicated times. They were then fixed and processed for indirect immunofluorescence staining with antibodies to α-tubulin (FITC, green) and for staining of DNA with propidium iodide (red). (**c**) Quantitation of mitotic progression. WTW1 and KDW1 cells were treated and analysed as in (b), and the percentage of cells in prometaphase, metaphase, anaphase, or telophase at the indicated times after release from nocodazole treatment was determined from examination of 200–300 cells of each line. (**d**) Immunostaining with antibodies to MAD2. WTW1 and KDW1 cells were treated with nocodazole, released into normal medium for 20 min, and then subjected to indirect immunostaining with antibodies to MAD2 (FITC, green) and to staining of DNA with propidium iodide (red). Representative cells are shown. Arrows indicate kinetochores positive for MAD2

Cleveland, 2000). At 20 min after release from nocodazole treatment, most WTW1 cells had already entered anaphase; all chromosomes were aligned at the metaphase plate and exhibited only faint staining for MAD2 (Figure 3d). In contrast, in most KDW1 cells at this time, some of the chromosomes had still not aligned at the metaphase plate and MAD2 staining was pronounced at the kinetochores of such misaligned chromosomes. Given that a single MAD2-positive unaligned chromosome is sufficient to activate the spindle assembly checkpoint (Nicklas, 1997), our observations suggest that prolonged activation of this checkpoint contributes to the mitotic delay observed in KDW1 cells. The kinase-inactive WARTS mutant may thus interfere with kinetochore function or assembly of the mitotic spindle, resulting in prolonged activation of the spindle assembly checkpoint and prometaphase delay. WARTS localizes to the mitotic spindle during mitotic phase (Nishiyama *et al*., 1999), and the peak of WARTS kinase activity coincided with the timing of prometaphase-to-metaphase progression (Figure 1d). These data suggest that activation of WARTS might play an important role in the regulation of events related to the spindle attachment to kinetochore and chromosome alignment.

DNA synthesis without cell division after prolonged activation of the spindle assembly checkpoint in KDW1 cells

Progression of tumors to a highly aneuploid state is thought to occur in at least two discrete steps. First, failure of the primary control of chromosome segregation or cytokinesis results in the generation of a tetraploid cell. Second, failure of a p53- and pRb-dependent surveillance mechanism that normally arrests such tetraploid cells in G_1 leads to aberrant DNA synthesis (Margolis *et al*., 2003). We have shown that prolonged activation of the spindle assembly checkpoint appears to be responsible for the pronounced mitotic delay in KDW1 cells and for allowing such cells to exit mitosis without undergoing cytokinesis, resulting in the formation of G_1 cells with a DNA content of 4N. We, therefore next determined whether the G_1 tetraploidy checkpoint prevents these cells from undergoing another round of DNA synthesis. To this end, we investigated the fate of cells treated with nocodazole to induce prolonged activation of the spindle assembly checkpoint. Asynchronous cells were treated with nocodazole for 12 h, and mitotic cells were then collected by the 'shake off' procedure and transferred to new dishes for further treatment with nocodazole. The cells that flattened back onto the culture dishes in the presence of nocodazole were analysed. The percentage of these cells with a DNA content of 8N was markedly greater for the KDW1 line than for the WTW1 line (Figure 4a), indicating that a substantial proportion of KDW1 cells with a DNA content of 4N underwent an additional round of DNA synthesis to yield a DNA content of 8N. Most KDW1-rev cells appeared to arrest with a DNA content of 4N. On the other hand, nocodazole-treated WTW1 cells showed a marked reduction in the proportion of cells with a DNA content of 4N that was concomitant with an increase in the size of the sub-G_1 population, indicating that a large number of WTW1 cells with a 4N DNA content underwent cell death as a result of the prolonged treatment with nocodazole. These results suggest that, in cells that have become tetraploid as a result of mitotic errors, overexpression of kinase-inactive WARTS induces abrogation of the G_1 tetraploidy checkpoint and that overexpression of wild-type WARTS induces cell death rather than G_1 arrest.

Role of WARTS in p53 induction at the G_1 tetraploidy checkpoint

To investigate why KDW1 cells with a DNA content of 4N fail to undergo G_1 arrest, we examined the expression of p53, a key player in activation of the G_1 tetraploidy checkpoint (Minn *et al*., 1996; Lanni and Jacks, 1998; Andreassen *et al*., 2001). Although p53 was accumulated in KDW1-rev cells treated with nocodazole for 26 h as described above, its abundance was markedly reduced in similarly treated KDW1 cells (Figure 4b). It was not possible to examine WTW1 cells in this experiment because most of these cells underwent apoptosis in response to prolonged nocodazole treatment as shown above (Figure 4a). These results suggest that abrogation of the G_1 tetraploidy checkpoint in KDW1 cells is due to a defect in the induction of p53. Overexpression of kinase-inactive WARTS thus induces not only activation of the spindle assembly checkpoint but also abrogation of the G_1 tetraploidy checkpoint, resulting in the development of polyploidy. It therefore appears that the kinase activity of WARTS plays important roles in both mitotic progression and the G_1 tetraploidy checkpoint.

Discussion

This study is the first demonstration that WARTS kinase is activated at the prometaphase/metaphase transition. Our data suggest that WARTS activation plays an important role in the regulation of spindle attachment to kinetochore and chromosome alignment. Thus, impairment of WARTS function leads to the activation of spindle assembly checkpoint. Although the function of the spindle assembly checkpoint is thought to be to ensure the correct assembly of a functioning mitotic spindle before exit from mitosis, the ability of cells to arrest in mitosis varies (Kung *et al*., 1990); many cell types thus undergo only a transient mitotic arrest and then exit mitosis without chromosome segregation. Consistent with these observations, we have shown here that cells expressing a kinase-inactive WARTS, KDW1 cells, frequently experience prolonged activation of the spindle assembly checkpoint and subsequently exit mitosis without cell division and therefore became tetraploid. Cells that have evaded mitotic arrest after activation of the spindle assembly checkpoint by treatment with an inhibitor of microtubule assembly have previously been shown to undergo p53-dependent

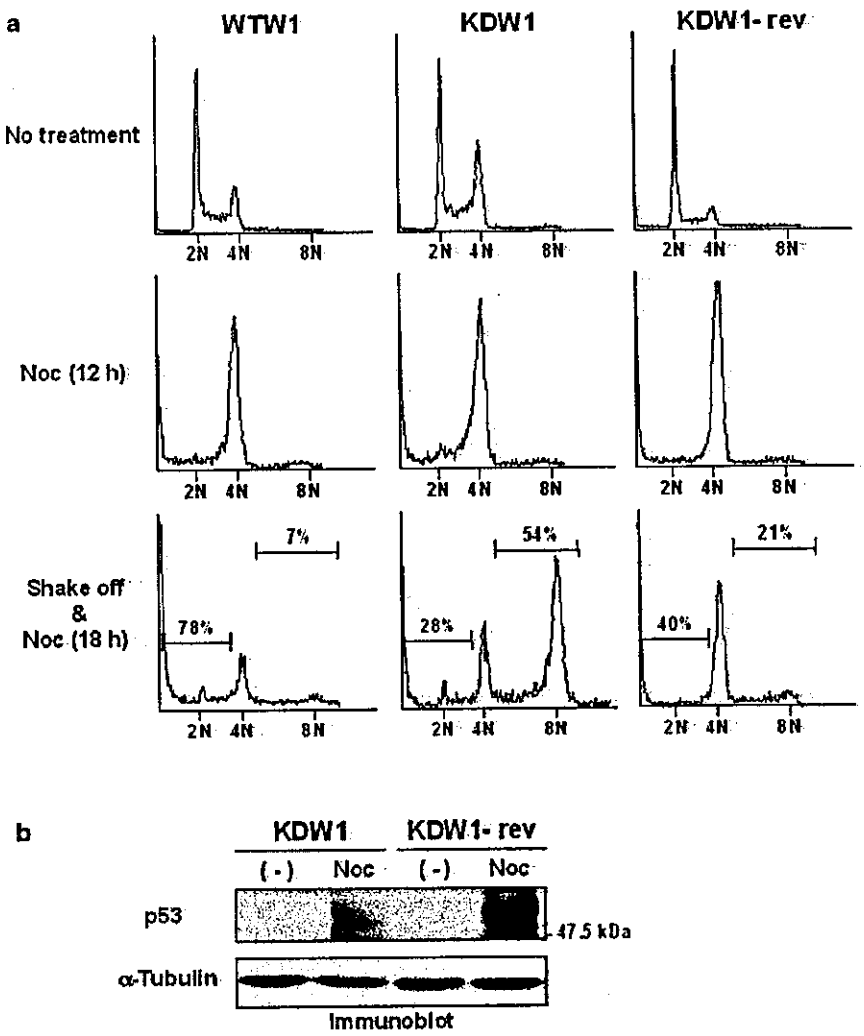

Figure 4 Role of WARTS in the G_1 tetraploidy checkpoint. (a) Asynchronous WTW1, KDW1, or KDW1-rev cells (upper panels) were treated with nocodazole for 12 h (middle panels), and mitotic cells were then collected by the shake-off procedure and transferred to new dishes for incubation for an additional 18 h with nocodazole (lower panels). The DNA content of attached cells was determined by flow cytometry. Percentages refer to the number of cells with a DNA content of <4N or >4N. (b) KDW1 and KDW1-rev cells were treated (or not) with nocodazole for 26 h as described in (a), and attached G_1 cells were then collected and lysed. Lysates were subjected to SDS–PAGE on a 10% gel followed by immunoblot analysis with antibodies to p53 (R-19, Santa Cruz) or to α-tubulin.

G_1 arrest (Minn *et al*., 1996; Lanni and Jacks, 1998). Moreover, cells treated with an inhibitor of actin assembly to induce failure of cytokinesis underwent p53-dependent G_1 arrest even when formation of the mitotic spindle and chromosome segregation proceeded normally, suggesting that tetraploidy *per se* leads to G_1 arrest (Andreassen *et al*., 2001). Our detection of a substantial population of KDW1 cells with a DNA content of 8N after prolonged activation of the spindle assembly checkpoint suggests that overexpression of the kinase-inactive WARTS mutant impaired G_1 tetraploidy checkpoint function. In fact, we further demonstrated that the induction of p53 was defective in nocodazole-treated KDW1 cells, indicating that the kinase activity of WARTS is required for p53 induction. This defect of p53 induction appears to be responsible for failure to activate the G_1 tetraploidy checkpoint and entry into subsequent S phase in KDW1 cells. We are currently investigating how the activated WARTS induces p53 accumulation when mitosis is failed.

Since the only one clone of kinase-inactive mutant was available in this study, it raises the possibility that overexpression of kinase-inactive WARTS might cause some additional effects in this clone other than simply interfering the function of the endogenous WARTS expressed in Rat 1 cells. However, the distribution of mutant WARTS is essentially the same as that of wild-type WARTS (Figure 1c), suggesting that mutants WARTS does not associate with some unexpected targets. Furthermore, KDW1-rev cells, which lost the mutant WARTS expression, showed the similar phenotypes to the parental Rat 1 cells. It is thus likely that the kinase-inactive WARTS inhibits endogenous WARTS in a dominant-negative manner.

It was previously reported that ectopic expression of WARTS in human cancer cells induces upregulation of BAX proteins and leads to apoptosis (Yang *et al.*, 2001; Xia *et al.*, 2002). In contrast, our study shows that overexpression of wild-type WARTS in Rat1 fibroblasts resulted in neither apoptosis nor cell cycle arrest. These discrepancies might be attributed to differences between cancer cells and normal cells. It should be noted that overexpression of wild-type WARTS in Rat1 fibroblasts (WDW1 cells) preferentially induced apoptosis when spindle damage was induced by nocodazole treatment, whereas KDW1-rev cells did not (Figure 4a). These differences in sensitivity of the two cell lines to nocodazole may be due to the differences in the expression levels of wild-type WARTS protein. These findings suggest that overactivation of WARTS kinase induces apoptosis in the presence of tumorigenic signals and cytotoxic stress such as spindle damage or DNA damage. Therefore, activation and/or overexpression of WARTS may provide a potential specific therapeutic approach for treating malignant tumors.

Overexpression of other mitotic kinases (Polo-like kinase 1, Aurora-A, Aurora-B) also induces mitotic failure concomitant with multinucleation and an increase in centrosome number, and the absence of p53-dependent checkpoint function exacerbates this phenotype (Meraldi *et al.*, 2002). In this regard, it thus appears that WARTS is unique in that it regulates not only mitotic progression but also p53-mediated checkpoint function. Inactivation of WARTS kinase alone thus possibly leads to genomic instability and development of tumors through mitotic failure, G_1 checkpoint abrogation, and the survival of abnormal cells.

Materials and methods

Cell culture and synchronization

Parental Rat1 cells and stable transfectants were cultured in DME-F12 medium supplemented with 10% fetal bovine serum without antibiotics. For cell synchronization in prometaphase, cells were incubated for 10 h with nocodazole (50 ng/ml) and then released into normal medium.

Generation of Rat1 cells stably expressing WARTS

Rat1 cells in six-well plates were transfected, with the use of FuGENE 6 (Roche), with the expression vector pUHG10-3 containing the cDNA for either wild-type or kinase-inactive forms of human WARTS. The kinase-inactive WARTS mutant (K734A) was constructed by replacing lysine 734 in the ATP-binding site with alanine. After 48 h, the cells were cultured in the presence of hygromycin B (0.2 mg/ml) (Wako), and antibiotic-resistant cell colonies were isolated 1 week later by ring cloning.

Immunofluorescence microscopy

Cells were grown in 35-mm dishes to ~70% confluence. Fixation and permeabilization were performed as previously described (Hirota *et al.*, 2000). After washing with PBS, the cells were incubated with primary antibodies including mouse monoclonal antibodies to Myc (9E10, Roche), mouse monoclonal antibodies to α-tubulin (B-5-1-2, Sigma), rabbit polyclonal antibodies to MAD2 (Marumoto *et al.*, 2003), rat polyclonal antibodies to α-tubulin (Novus Biologicals) or to γ-tubulin (Sigma). Immune complexes were detected with fluorescein isothiocyanate (FITC) — conjugated antibodies to mouse immunoglobulin G (IgG), FITC-conjugated antibodies to rabbit IgG (Amersham Pharmacia), or Alexa 568-conjugated antibodies to rat IgG (Molecular Probes). The stained cells were mounted and observed as previously described (Hirota *et al.*, 2000).

Immune-complex kinase assay

Cells were lysed on ice for 20 min in a solution containing 0.5% NP-40, 100 mM NaCl, 2 mM EDTA, 5 mM EGTA, 50 mM HEPES-KOH (pH 7.4), 10 mM $MgCl_2$, 5 mM $MnCl_2$, 5 mM KCl, 100 μM leupeptin, 1 μM pepstatin, 100 μM Tosyl Lysine Chloromethyl Ketone (TLCK), 100 nM okadaic acid, 2 mM benzamidine, and 1 mM dithiothreitol. The lysate was centrifuged at 18000*g* for 20 min, and portions of the supernatant (0.2–2.0 mg/ml) were incubated at 4°C first for 2 h with antibodies to Myc (9E10) and then, after the addition of protein G-Sepharose beads (Amersham Pharmacia), for an additional 90 min. The beads were then isolated by centrifugation, washed with cell lysis buffer, and subjected to the *in vitro* kinase assay. Kinase reactions were performed for 30 min at 30°C in a final volume of 30 μl containing 20 mM Tris-HCl (pH 7.4), 10 mM $MgCl_2$, 10 μCi of [γ-^{32}P]ATP (3000 Ci/mmol) (Amersham Pharmacia), and 1 μM microcystin. The phosphorylated proteins were resolved by SDS–PAGE on a 5–20% acrylamide-gradient gel and visualized by autoradiography.

Acknowledgements
We thank all colleagues in Department of Tumor Genetics and Biology, Graduate School of Medical Sciences, Kumamoto University for helpful discussion. We are also grateful to members of the Gene Technology Center and General Research Institute in Kumamoto University for their important contributions to the experiments. This work was supported by a grant for cancer research from the Ministry of Education, Science and Culture of Japan (H. Saya).

References

Amon A. (1999). *Curr. Opin. Genet. Dev.*, **9**, 69–75.
Andreassen PR, Lohez OD, Lacroix FB and Margolis RL. (2001). *Mol. Biol. Cell*, **12**, 1315–1328.
Hanks SK, Quinn AM and Hunter T. (1988). *Science*, **241**, 42–52.
Hirota T, Morisaki T, Nishiyama Y, Marumoto T, Tada K, Hara T, Masuko N, Inagaki M, Hatakeyama K and Saya H. (2000). *J. Cell Biol.*, **149**, 1073–1086.
Hisaoka M, Tanaka A and Hashimoto H. (2002). *Lab. Invest.*, **82**, 1427–1435.
Justice RW, Zilian O, Woods DF, Noll M and Bryant PJ. (1995). *Genes Dev.*, **9**, 534–546.
King RW, Peters JM, Tugendreich S, Rolfe M, Hieter P and Kirschner MW. (1995). *Cell*, **81**, 279–288.
Kung AL, Sherwood SW and Schimke RT. (1990). *Proc. Natl. Acad. Sci. USA*, **87**, 9553–9557.

Lanni JS and Jacks T. (1998). *Mol. Cell Biol.*, **18**, 1055–1064.
Margolis RL, Lohez OD and Andreassen PR. (2003). *J. Cell Biochem.*, **88**, 673–683.
Marumoto T, Honda S, Hara T, Nitta M, Hirota T, Kohmura E and Saya H. (2003). *J. Biol. Chem.*, **278**, 51786–51795.
Meraldi P, Honda R and Nigg EA. (2002). *EMBO J.*, **21**, 483–492.
Minn AJ, Boise LH and Thompson CB. (1996). *Genes Dev.*, **10**, 2621–2631.
Nicklas RB. (1997). *Science*, **275**, 632–637.
Nishiyama Y, Hirota T, Morisaki T, Hara T, Marumoto T, Iida S, Makino K, Yamamoto H, Hiraoka T, Kitamura N and Saya H. (1999). *FEBS Lett.*, **459**, 159–165.
Shackney SE, Smith CA, Miller BW, Burholt DR, Murtha K, Giles HR, Ketterer DM and Pollice AA. (1989). *Cancer Res.*, **49**, 3344–3354.
Shah JV and Cleveland DW. (2000). *Cell*, **103**, 997–1000.
St John MA, Tao W, Fei X, Fukumoto R, Carcangiu ML, Brownstein DG, Parlow AF, McGrath J and Xu T. (1999). *Nat. Genet.*, **21**, 182–186.
Tao W, Zhang S, Turenchalk GS, Stewart RA, St John MA, Chen W and Xu T. (1999). *Nat. Genet.*, **21**, 177–181.
Toyn JH and Johnston LH. (1994). *EMBO J.*, **13**, 1103–1113.
Tugendreich S, Tomkiel J, Earnshaw W and Hieter P. (1995). *Cell*, **81**, 261–268.
Xia H, Qi H, Li Y, Pei J, Barton J, Blackstad M, Xu T and Tao W. (2002). *Oncogene*, **21**, 1233–1241.
Yang X, Li DM, Chen W and Xu T. (2001). *Oncogene*, **20**, 6516–6523.
Yasui Y, Amano M, Nagata K, Inagaki N, Nakamura H, Saya H, Kaibuchi K and Inagaki M. (1998). *J. Cell Biol.*, **143**, 1249–1258.

9

Critical Roles for the Fas/Fas Ligand System in Postinfarction Ventricular Remodeling and Heart Failure

Yiwen Li, Genzou Takemura, Ken-ichiro Kosai, Tomoyuki Takahashi, Hideshi Okada, Shusaku Miyata, Kentaro Yuge, Satoshi Nagano, Masayasu Esaki, Ngin Cin Khai, Kazuko Goto, Atsushi Mikami, Rumi Maruyama, Shinya Minatoguchi, Takako Fujiwara, Hisayoshi Fujiwara

Abstract—In myocardial infarction (MI), granulation tissue cells disappear via apoptosis to complete a final scarring with scanty cells. Blockade of this apoptosis was reported to improve post-MI ventricular remodeling and heart failure. However, the molecular biological mechanisms for the apoptosis are unknown. Fas and Fas ligand were overexpressed in the granulation tissue at the subacute stage of MI (1 week after MI) in mice, where apoptosis frequently occurred. In mice lacking functioning Fas (*lpr* strain) and in those lacking Fas ligand (*gld* strain), apoptotic rate of granulation tissue cells was significantly fewer compared with that of genetically controlled mice, and post-MI ventricular remodeling and dysfunction were greatly attenuated. Mice were transfected with adenovirus encoding soluble Fas (sFas), a competitive inhibitor of Fas ligand, on the third day of MI. The treatment resulted in suppression of granulation tissue cell apoptosis and produced a thick, cell-rich infarct scar containing rich vessels and bundles of smooth muscle cells with a contractile phenotype at the chronic stage (4 weeks after MI). This accompanied not only alleviation of heart failure but also survival improvement. However, the sFas gene delivery during scar tissue phase was ineffective, suggesting that beneficial effects of the sFas gene therapy owes to inhibition of granulation tissue cell apoptosis. The Fas/Fas ligand interaction plays a critical role for granulation tissue cell apoptosis after MI. Blockade of this apoptosis by interfering with the Fas/Fas ligand interaction may become one of the therapeutic strategies against chronic heart failure after large MI. (*Circ Res.* 2004;95:627-636.)

Key Words: apoptosis ■ gene therapy ■ heart failure ■ myocardial infarction ■ remodeling

Large myocardial infarction (MI) causes severe chronic heart failure with unfavorable remodeling of the left ventricle (LV), which is characterized by a ventricular dilatation and diminished cardiac performance.[1] The magnitude of acute MI, which is determined within several hours after an attack of MI,[2] is the most critical determinant of subsequent heart failure. However, many other factors, such as late death or hypertrophy of cardiomyocytes, fibrosis, and the expression of various cytokines, are associated with the disease progression.[3–6] Cardiomyocyte death resulting from apoptosis during chronic heart failure may play an important role in the disease progression,[7–9] although its role is still unclear because of a low incidence.[10–13] In contrast, nonmyocytes in the infarct area, such as infiltrating inflammatory cells during the acute stage and granulation tissue cells during the subacute stage of MI, do die via apoptosis as we reported previously.[14] Granulation tissue in particular contains an abundance of neovasculature, myofibroblasts, and macrophages. We reported recently that inhibition of granulation tissue cell apoptosis by use of Boc-Asp-fmk, a pancaspase inhibitor, significantly improved LV remodeling and heart failure at the chronic stage of MI.[15] However, the molecular mechanisms of this apoptosis have not been determined, although a dependency on caspases is recognized.

Fas/Fas ligand interaction is an important trigger for apoptosis in many cell types, particularly cells related to the immune system.[16] Because MI ensues inflammation and post-MI granulation tissue contains chronic inflammatory cells, we hypothesize that the Fas/Fas ligand system is involved in the apoptosis of granulation tissue cells. In the present study, we first report that the Fas/Fas ligand system is activated in post-MI granulation tissue cells and significantly influences the postinfarct process. Next, we show that inhibition of the Fas/Fas ligand system by delivery of the gene for soluble Fas, a competitive inhibitor of Fas/Fas ligand interaction,[17] during the subacute stage of MI could potentially prevent post-MI heart failure at the chronic stage.

Methods

Experimental MI in Mice

The study was approved by our institutional animal research committee. MI was created in male C57BL/6J wild-type mice and

Original received March 19, 2004; revision received July 7, 2004; accepted July 27, 2004.

From the Second Department of Internal Medicine (Y.L., G.T., H.O., S. Miyata, M.E., R.M., S. Minatoguchi, H.F.) and the Department of Gene Therapy and Regenerative Medicine (K.-i.K., T.T., K.Y., S.N., M.E., N.C.K., K.G., A.M.), Gifu University School of Medicine, Gifu; and the Department of Food Science (T.F.), Kyoto Women's University, Kyoto, Japan.

Correspondence to Hisayoshi Fujiwara, MD, PhD, Second Department of Internal Medicine, Gifu University School of Medicine, 1-1 Yanagido, Gifu 502-1194 Japan. E-mail gifuim-gif@umin.ac.jp

Circulation Research is available at http://www.circresaha.org DOI: 10.1161/01.RES.0000141528.54850.bd

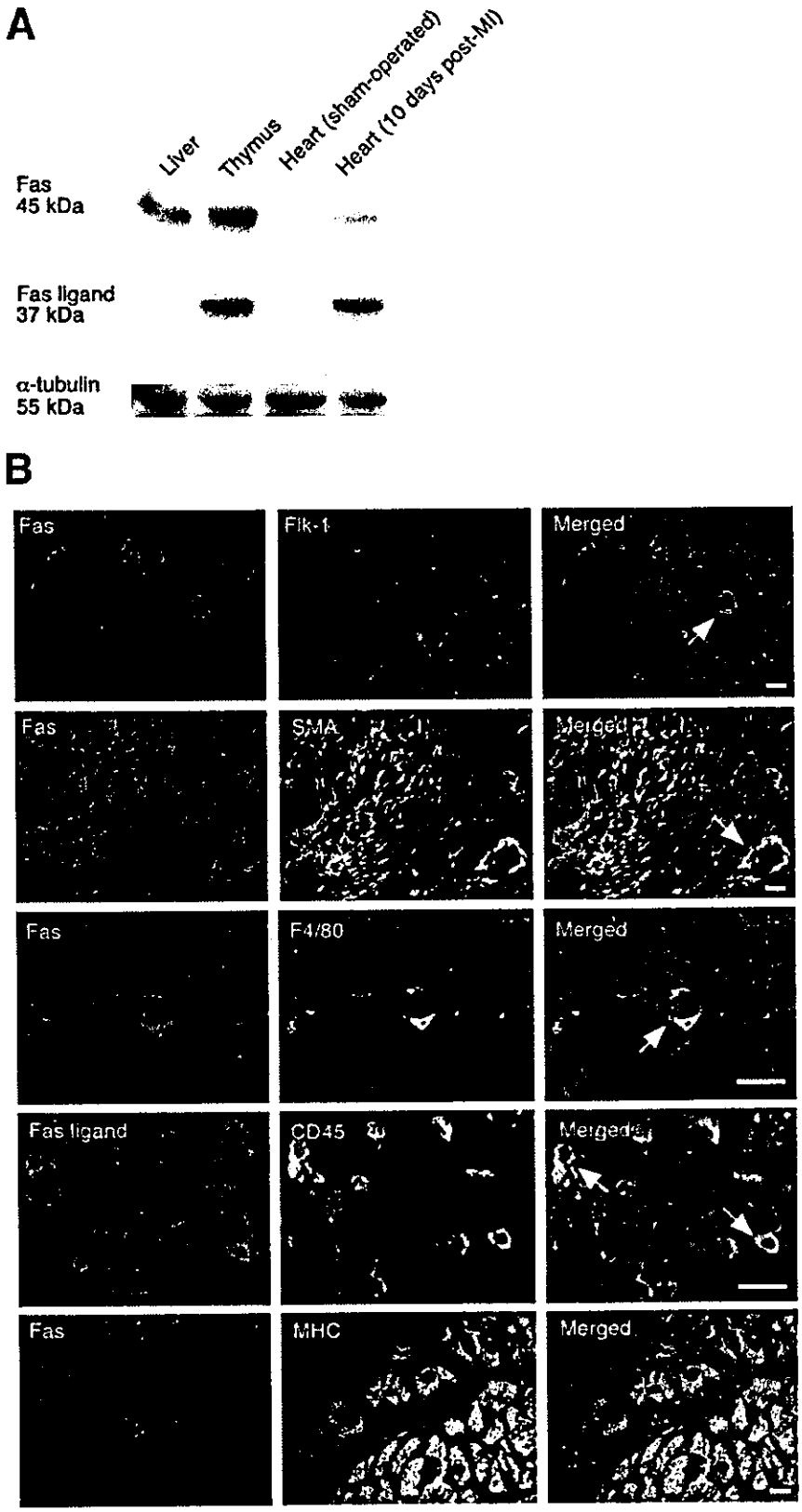

Figure 1. Augmented expression of Fas and Fas ligand in the infarct area 10 days after MI. A, Western blots for Fas and Fas ligand in normal liver, normal thymus, sham-operated heart, and heart with 10-day-old MI. Expression of both Fas and Fas ligand was significantly augmented in the heart with MI compared with the sham-operated heart. α-tubulin was a loading control. B, Double immunofluorescence for Fas or Fas ligand (red) combined with Flk-1, α-SMA, F4/80, CD34, or cardiac myosin heavy chain (MHC; green), under a confocal microscope. Fas positivity was seen in endothelial cells, vascular smooth muscle cells, extravascular myofibroblasts (asterisk), macrophages, and leukocytes but not in cardiomyocytes, whereas Fas ligand positivity was limited to leukocytes. Arrows and an asterisk indicate double-positive cells. Bars=20 μm.

syngenetic *lpr* mice and *gld* mice (Clea Japan; Shizuoka, Japan) at 12 weeks of age by ligating the left coronary artery as described.[18] In sham-operated mice, the suture was passed but not tied. Animals were killed 2 days, 10 days, 4 weeks, or 10 weeks after surgery.

Recombinant Adenoviral Vectors

Replication-incompetent adenoviral vector that ubiquitously and strongly expresses a chimeric fusion protein of extracellular region of mouse Fas and the Fc region of human IgG_1 (mFas-Fc), that is,

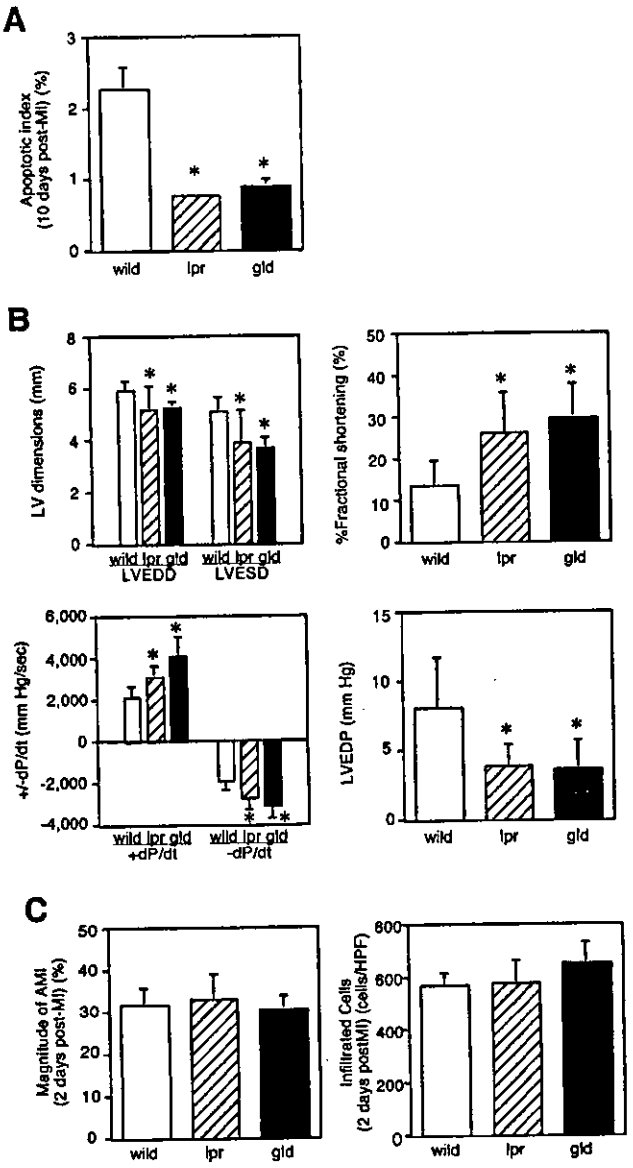

Figure 2. Modified post-MI ventricular remodeling and dysfunction in *lpr* and *gld* mice. A, Apoptotic index on the basis of a TUNEL assay in granulation tissue 10 days after MI in wild-type, *lpr*, and *gld* mice. *$P<0.05$ compared with wild-type. B, Anatomical and hemodynamic data for the hearts with a 4-week-old MI obtained from echocardiography and cardiac catheterization. *$P<0.05$ compared with wild-type mice. LVEDD indicates LV end-diastolic dimension; LVESD, LV end-systolic dimension. C, Magnitude of acute myocardial infarct (2-day-old MI) evaluated as the percentage of infarct area to total LV area in wild-type, *lpr*, and *gld* mice.

soluble Fas (sFas), was generated as follows. Adenoviral vector plasmid pAd-sFas, which comprises the cytomegalovirus immediate early enhancer, a modified chicken β-actin promoter and the extracellular region of mouse Fas (sFas) cDNA (Ad.CAG-sFas) was constructed by the in vitro ligation method (gift from Dr Mark A. Kay, Stanford University School of Medicine, California) as described previously.[19] Plasmid pFAS-FcII was generously provided by Dr S. Nagata (Osaka University Graduate School of Medicine, Japan).[20] Control Ad-LacZ was prepared as reported previously.[21]

On day 3 of MI, the sFas gene or LacZ gene was systemically delivered to mice by injection of Ad.CAG-sFas or Ad-LacZ (1×10^9 plaque-forming units[pfu]/mouse) into the hindlimb muscles.

Measurement of the sFas Level in Plasma

The plasma concentration of sFas was measured by detecting human IgG-Fc using an ELISA kit (Institute of Immunology).

Physiological Studies

Echocardiograms were recorded with an echocardiographic system (Aloka) equipped with a 7.5-MHz imaging transducer at 4 or 10 weeks after MI. After cardiac echocardiography, the right carotid artery was cannulated with a micromanometer-tipped catheter (SPR 407; Millar Instruments) and advanced into the aorta and then into the LV for recording pressure and ±dP/dt.

Histological Analysis

After measurements, hearts were removed and cut into 2 transverse slices, and the basal specimens were fixed with 10% buffered formalin and embedded in paraffin. Sections 4-μm thick were stained with hematoxylin-eosin or Masson's trichrome. Quantitative assessments including cell size, cell population, and fibrotic area were performed using multipurpose color image processor LUZEX F (Nireco).

Western Blotting

An immunoprecipitation assay of the lysate of heart tissues was performed with Ultra-Link Biosupport medium (Pierce) using anti-Fas antibody and anti-Fas ligand antibody (both from BD Transduction Laboratories). Subsequently, the isolated protein was analyzed by Western blotting using the same antibodies. Sham-operated hearts 10 days after surgery, hearts with 10-day-old MI, normal thymus, and normal livers (n=5 each) were subjected to the assay.

Active forms of caspase-8 and caspase-3 were detected, respectively, using the primary antibody against caspase-8 (H-134; Santa Cruz Biotechnology) and caspase-3 (H-277; Santa Cruz Biotechnology) in sham-operated mice and LacZ gene-treated and sFas gene-treated mouse hearts with 10-day-old MI (n=5 each).

Hindlimb muscles of mice injected with Ad-LacZ or Ad.CAG-sFas 7 days earlier (n=3 each) were subjected to Western blot for exogenous sFas by anti-human IgG antibody (DAKO).

Immunohistochemical Analysis

The sections, 4-μm-thick deparaffinized sections or 8-μm-thick cryosections from the apical half of the ventricle, were incubated with anti-Fas antibody, anti-Fas ligand antibody, anti-Flk-1 antibody (Santa Cruz Biotechnology), anti–α-smooth muscle actin (SMA) antibody (Sigma), anti-CD45 antibody (Pharmingen), antimacrophage antibody (F4/80; Biomedicals AG), or anticardiac myosin heavy chain antibody (Santa Cruz Biotechnology). The ABC kit (DAKO) was used for the immunostaining of the deparaffinized sections with diaminobenzidine as the chromogen. For immunofluorescence of cryosections, Alexa Fluor 568 and 488 (Molecular Probes) were the secondary antibodies. Nuclei were counterstained with hematoxylin or Hoechst 33342. Sections were observed under a light, or confocal, microscope (LSM510; Zeiss).

In Situ Nick End-Labeling (TUNEL) and DNA Gel Electrophoresis

The TUNEL assay was performed in sections using an ApopTag kit (Intergene) principally according to the instructions of the supplier. Mammary tissue of mice was used as the positive control.

DNA extraction from cardiac tissue and subsequent electrophoresis were performed as reported previously.[14]

Electron Microscopy

Two to 3 animals in each group were used exclusively for transmission electron microscopic examinations after the hemodynamic examination. After perfusion fixation with phosphate-buffered 2.5% glutaraldehyde, pH 7.4, for 30 minutes, they were immersion-fixed in the same fixative overnight, postfixed with 1% osmium tetroxide for 1 hour, dehydrated through a graded series of ethanol, and embedded in Epon medium. Ultrathin sections were stained with

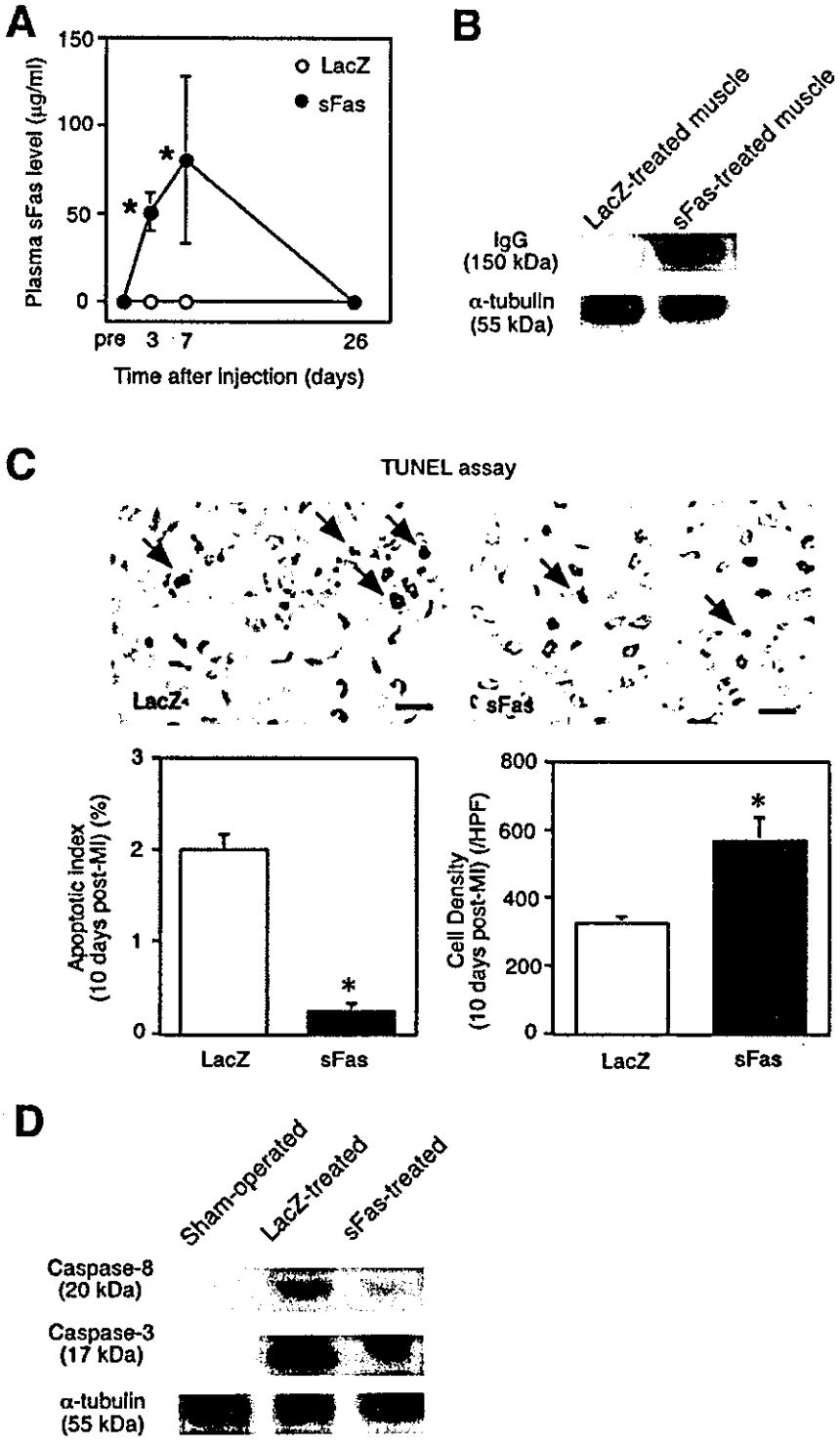

Figure 3. Effects of sFas gene delivery on granulation tissue cell apoptosis during the subacute stage of MI. A, Time course of exogenous sFas levels in the plasma of mice. ● indicates sFas gene-treated mice; ○, LacZ gene-treated mice (n=6 each). *$P<0.05$ compared with the value for the LacZ gene-treated mice at the corresponding time point. B and C, Photomicrographs of granulation tissue used for TUNEL assays: left, LacZ gene-treated mouse heart; right, sFas gene-treated mouse heart. Arrows indicate TUNEL-positive cells. Bars=10 μm. Graphs showing the apoptotic index on the basis of TUNEL (right) and cell population of granulation tissue (left) of each group. *$P<0.05$. D, α-tubulin was a loading control.

uranyl acetate and lead citrate and observed in an electron microscope (H700; Hitachi).

Statistical Analysis

Values are shown as mean±SEM. Analyses of survival after the third or tenth day after MI were performed using the Kaplan–Meier method with the log-rank Cox–Mantel method. The significance of differences was evaluated with Student *t* test, and a difference at $P<0.05$ was considered significant.

Results

Expression of Fas and Fas Ligand in Granulation Tissue Cells During MI

We first examined the expression of Fas and Fas ligand in granulation tissue of the heart at the subacute stage of MI (10 days after MI and 10 days after sham operation; n=5 each). Western blot analysis of the cardiac tissue revealed an

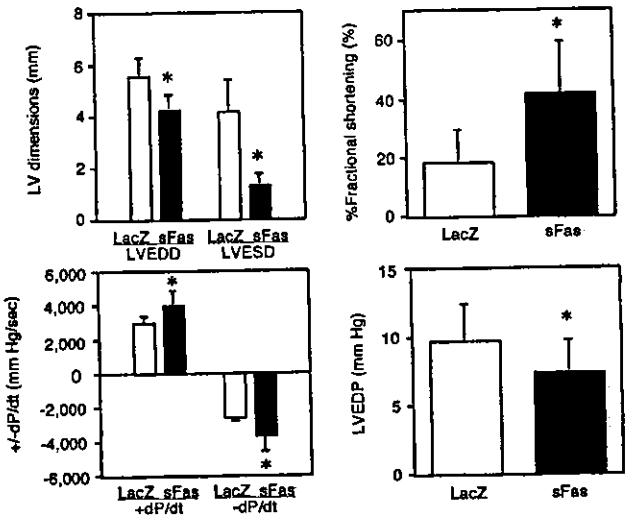

Figure 4. Effects of sFas gene delivery on hearts at the chronic stage of MI (4 weeks after MI). Graphs show anatomical and hemodynamic data obtained from echocardiography and cardiac catheterization. *$P<0.05$ compared with LacZ gene-delivered mice. LVEDD indicates LV end-diastolic dimension; LVESD, LV end-systolic dimension.

augmented expression of Fas and Fas ligand in the heart with MI (Figure 1A). Under a confocal microscope, Fas was identified on the plasma membrane of endothelial cells (Fas positivity 81±2.9% of the endothelial cells), vascular smooth muscle cells (69±2.0%), extravascular myofibroblasts (45±2.9%), macrophages (79±3.2%), and leukocytes (73±3.6%), whereas Fas ligand was found only on the plasma membrane of leukocytes (Fas ligand positivity 21±2.7% of the CD45-positive cells; Figure 1B). Under the present staining conditions, neither Fas nor Fas ligand was detected on the surface of cardiomyocytes, even at the border of the infarct area (Figure 1B).

Apoptosis was detectable by TUNEL assay in noncardiomyocytes of granulation tissue but never in cardiomyocytes. We failed to detect a ladder pattern on DNA gel electrophoresis in the tissue from hearts with 10-day-old MI (data not shown). This failure was compatible with previous reports[14,22] and was probably attributable to the relatively low incidence of apoptotic cells. Electron microscopy confirmed this finding, being compatible with previous studies:[14,15] apoptosis of noncardiomyocytes and no apoptosis of cardiomyocytes (data not shown).

Attenuated Postinfarction Heart Failure in Mice with Nonfunctioning Fas and Fas Ligand

MI was induced in animals with a nonfunctioning Fas (*lpr* strain: *fas*$^{-/-}$; n=10),[23] those with a nonfunctioning Fas ligand (*gld* strain: *fas ligand*$^{-/-}$; n=10),[24] and in the syngenetic control mice (C57BL/6J strain; n=10). The lack of Fas and Fas ligand was confirmed, respectively, in the hearts of the *lpr* strain and the *gld* strain mice 10 days after MI (data not shown). On the basis of the TUNEL assay, granulation tissue cell apoptosis in surviving mice with 10-day-old MI was significantly suppressed in the nonfunctioning Fas/Fas ligand strains (0.74±0.02% in the *lpr* strain [n=9] and 0.88±0.06% in the *gld* strain [n=9]) compared with the control (2.3±0.16%; n=8; Figure 2A). Next, MI was similarly evoked in the *lpr* strain, *gld* strain, and control (n=10 each), and followed up for 4 weeks. At the chronic stage (4 weeks after MI), echocardiographic and hemodynamic examinations of the surviving mice (9 *lpr* mice, 10 *gld* mice, and 7 control mice) revealed a significant attenuation of LV remodeling and improvement of LV dysfunction in the *lpr* and *gld* strains, compared with the control (Figure 2B).

To check the possible difference in magnitude of acute MI between the control and nonfunctioning Fas/Fas ligand mice, we histologically measured the acute infarct size 2 days after MI (n=6 each). There was no difference in the percentage of MI in LV area among the groups (Figure 2C). Also, there was no difference in the degree of acute inflammatory cell infiltration at the periphery of the 2-day-old infarct area (Figure 2C).

Inhibition of Granulation Tissue Cell Apoptosis by sFas, an Inhibitor of Fas-Mediated Apoptosis

MI was induced in 12-week-old male C57BL/6J mice, and Ad.CAG-sFas (10^9 pfu/mouse) was delivered systemically through injection into the hindlimbs on the third day after MI (n=10) when cardiomyocyte necrosis was already completed. The control gene was LacZ cDNA (Ad.CAG-LacZ; n=10). In the sFas gene–delivered mice, the plasma level of exogenous sFas reached 51.0±11.0 μg/mL and 80.7±4.7 μg/mL, respectively, 3 and 7 days after the injection (6 and 10 days after MI), when the infarct area consisted of granulation tissue (Figure 3A); these levels might be sufficiently high when considering that in humans, the normal level of plasma sFas is ≈2 ng/mL.[25] However, the exogenous sFas was undetectable in the plasma at 4 weeks after MI. We confirmed expression of exogenous sFas by Western blotting for human IgG in the hindlimb muscles injected with Ad.CAG-sFas 7 days earlier, but it was not detected in those treated with Ad-LacZ (Figure 3B).

The sFas gene treatment significantly reduced the incidence of TUNEL-positive cells in the infarct area consisting of granulation tissue (Figure 3C); the apoptotic index on the basis of TUNEL in the infarct area of the treated mice 10 days after MI was 0.24±0.09% compared with 2.0±0.18% for the control mice. Active forms of caspase-8 and caspase-3 were detected not in the sham-operated mouse hearts but in the hearts with 10-day-old MI. However, these signals were apparently attenuated in the hearts treated with the sFas gene (Figure 3D). The noncardiomyocyte population in the infarct area was significantly greater in the sFas-treated mice (569±67 cells/high-power field [HPF]) than in the LacZ-treated mice (324±19 cells/HPF; Figure 3C). The number of vessels, the %area of myofibroblasts, and the number of macrophages in the infarct was significantly greater in the sFas-treated group than in the LacZ-treated group: vessels (vessels/HPF) 231±19 versus 168±16, $P=0.0022$; myofibroblasts (%) 31.5±6.4 versus 17.8±2, $P=0.0076$; and macrophages (cells/HPF) 7.5±0.66 versus 4.5±0.38, $P=0.0024$. These findings suggest that the inhibition of apoptosis through the blocking Fas/Fas ligand interaction resulted in preservation of the postinfarct granulation tissue cell population.

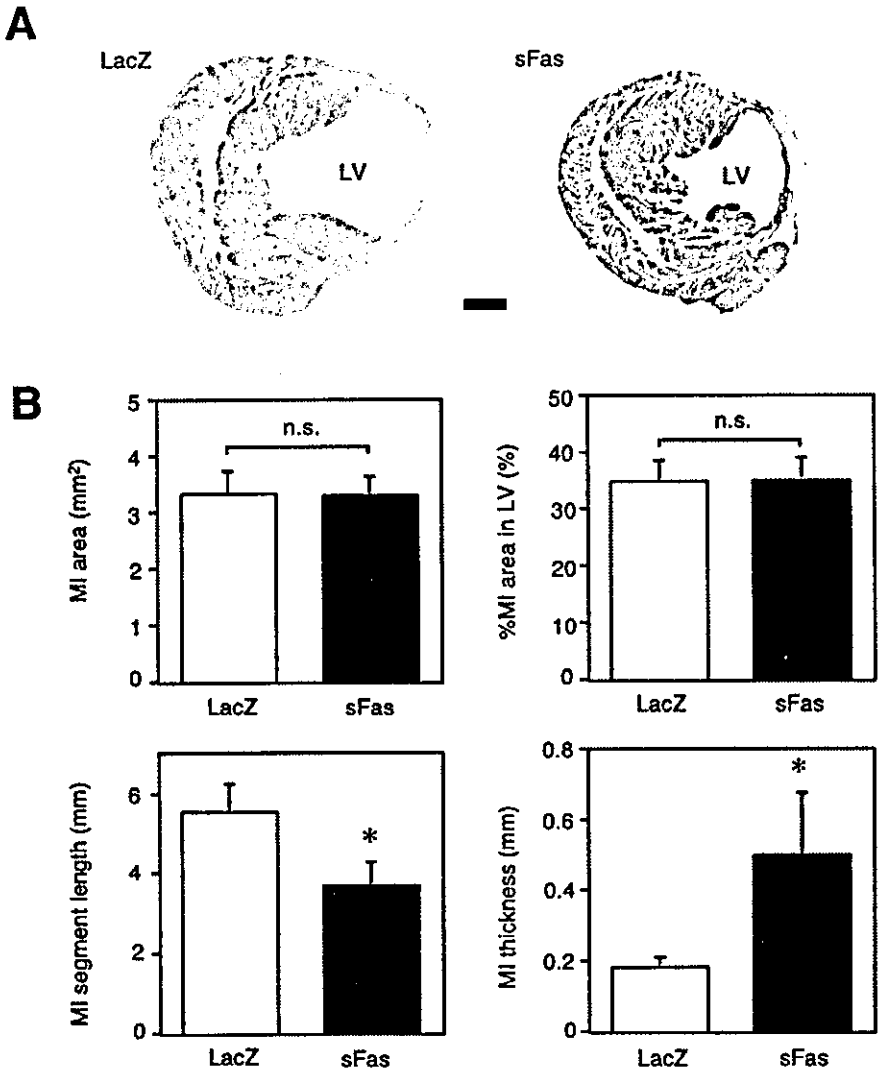

Figure 5. Effects of sFas gene delivery on hearts at the chronic stage of MI (4 weeks after MI). A, Transverse sections of hearts with 4-week-old MI; hematoxylin-eosin stain. Bar=1 mm. B, Graphs showing the absolute infarct area (μm^2); the percentage of the infarct area in total LV area (%); the length of the infarct segment (the inner circumferential length; μm); and the thickness of the infarct wall. *$P<0.05$ compared with the LacZ gene-delivered mice.

Improvement of Postinfarction LV Remodeling and Heart Failure by the sFas Gene Delivery

The influence of the sFas gene therapy was examined 4 weeks after MI (sFas gene [n=8] and LacZ gene [n=6]). At the chronic stage of MI, the LacZ-treated mice showed severe LV remodeling with a marked LV dilatation accompanying a thin infarct segment and signs of decreased cardiac function: decreased LV%FS and ±dP/dt; and an increased LV end-diastolic pressure. Gene delivery on the third day of MI resulted in a significant improvement of each of these conditions (Figure 4). Systemic blood pressure and heart rate were similar between the LacZ-treated and sFas-treated groups. Treatment with the sFas gene in normal mice did not cause any hemodynamic alteration or morphological change in the hearts compared with the LacZ treatment (n=5 each; data not shown).

Necropsy of the hearts of mice at 4 weeks after MI revealed a severely dilated LV cavity with a thin infarct wall in the LacZ-treated group. However, this unfavorable LV remodeling appeared attenuated in the sFas-treated group (Figure 5A). The absolute infarct size and proportion of infarct area to total LV area were similar between the LacZ-treated and sFas-treated mice at 4 weeks after MI (Figure 5B). Interestingly, the wall thickness of the infarct segment was greater, whereas the inner circumferential length of the infarct segment was smaller in the sFas-treated mice (Figure 5B). This indicated that the remodeling of the infarct wall expanding in the coronal directions was significantly suppressed in the sFas-treated mice.

The 4-week-old infarct area of the LacZ-treated mice was replaced by fibrous scar tissue (Figure 6A). However, that of the sFas-treated mice contained not only collagen fibers and fibroblasts but also many small vessels and abundant extravascular α-SMA–positive cells (myofibroblasts). The population of noncardiomyocytes in the old infarct area was significantly greater in the sFas-treated mice (390±9 cells/HPF in the sFas group versus 259±9 cells/HPF in the control) and so was that of vessels (165±7 vessels/HPF in the sFas group versus 114±7 vessels/HPF in the control; Figure 6A). The percent area of extravascular α-SMA–positive cells was significantly greater in the sFas-treated group (18±1.7%) than in the LacZ-treated group (7.6±1.6%). Some α-SMA–positive cells accumulated and formed bundles running parallel to the surviving cardiomyocytes. Such bundles were not

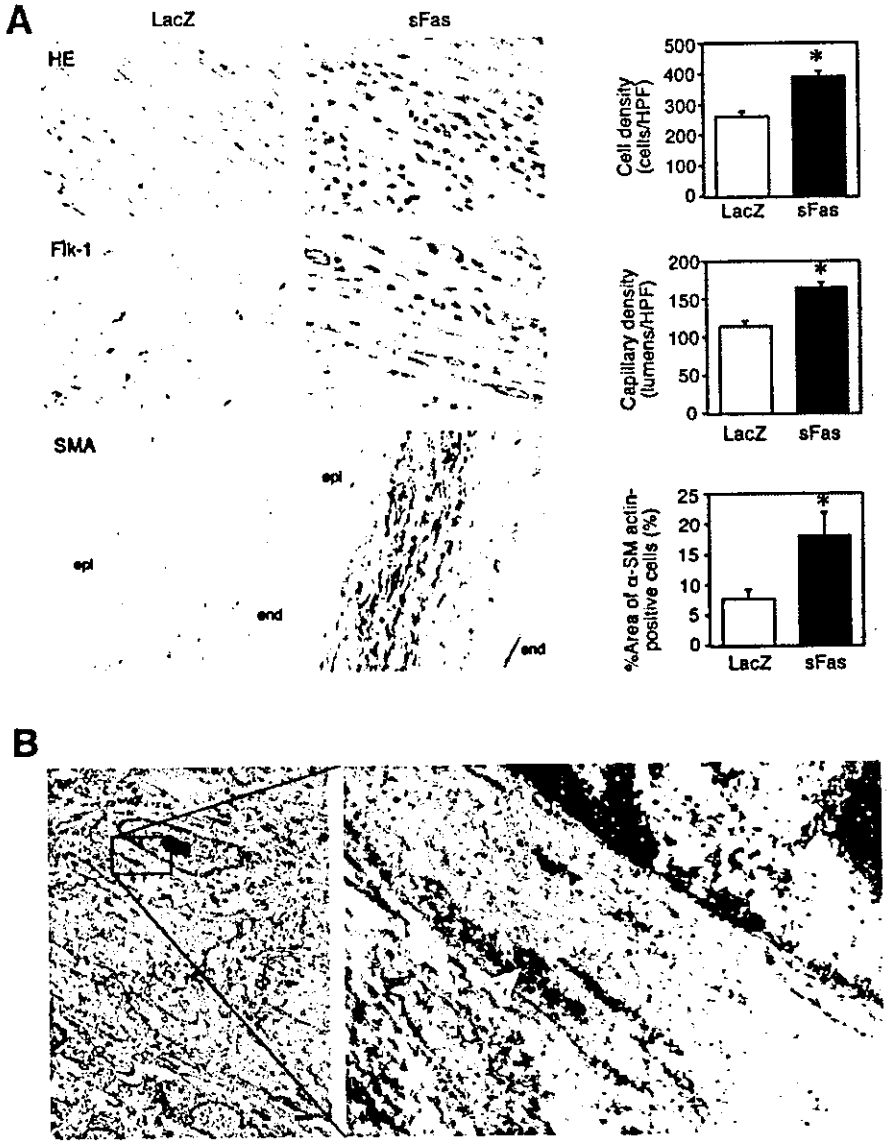

Figure 6. Effects of sFas gene delivery on cardiac histology and ultrastructure at the chronic stage of MI (4 weeks after MI). A, Photographs of histological and immunohistochemical preparations with graphs showing morphometrical data: the cell population of nonmyocytes in old infarct areas (cells/HPF); the vessel population in old infarct areas (vessels/HPF); and the percent areas of α-SMA–positive cells (%). *$P<0.05$ compared with the LacZ gene–delivered mice. B, Bundles of cells found in extravascular areas were found to be smooth muscle cells with a contractile phenotype under the electron microscope. The right panel is a highly magnified photograph of the squared portion of the neighboring panel showing densely packed myofilaments and dense bodies (arrows) in the cytoplasm. Bar=1 μm.

observed in the infarct wall of the LacZ-treated mice. However, macrophages were scarce even in the infarct area of the sFas-treated mouse hearts, and the incidence (1.7±0.62 cells/HPF) was similar to that in the LacZ-treated mice (1.3±0.56 cells/HPF; $P=0.6964$). The size of cardiomyocytes in the noninfarct area, which was measured as the transverse diameter, was significantly greater in the LacZ-treated mice (17.7±0.3 μm) than sFas-treated (14.0±0.7 μm) mice, suggesting that the compensatory hypertrophy of cardiomyocytes was more developed in the LacZ-treated mice. There was no special difference in thickness or in the degree of fibrosis of the noninfarct LV wall between the groups. No histological abnormality was found in the extracardiac organs such as lungs, liver, intestines, and kidneys of the sFas-treated mice.

Under an electron microscope, 4-week-old infarct areas of LacZ-treated mouse hearts contained fibroblasts/myofibroblasts (mostly fibroblasts), scanty small vessels, and very few macrophages that were surrounded by massive collagen fibrils, being consistent with a scar tissue. However, those of the sFas-treated hearts contained more abundant cell components. They showed not only numerous fibroblasts/myofibroblasts and small vessels but also mature smooth muscle cells with the contractile phenotype. These smooth muscle cells made bundles in the extravascular areas. The cytoplasms of the smooth muscle cells were tightly filled with thin filaments and contained many dense bodies (Figure 6B). The bundles of such smooth muscle cells were identical to the mass of α-SMA–positive cells that had appeared under the light microscope.

Influence of the sFas Gene Delivery on Postinfarction Survival

Using other litters of mice that were alive on the third day of MI (n=40), the survival was followed up for a period of 10 weeks. Eighteen mice underwent the sFas gene therapy and 22 the LacZ gene therapy. The survival rate was 55% in the control and 83% in the sFas-treated group at 10 weeks after MI ($P=0.0834$; Figure 7). Although the difference was not significant, it was notable that in case of

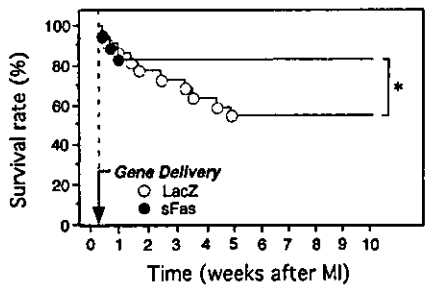

Figure 7. Survival of post-MI mice followed up for 10 weeks. ○ indicates LacZ gene treatment (n=20); ●, sFas gene treatment (n=18). *P=0.0834 (later than the third day of MI) or P=0.0389 (later than the tenth day of MI).

the sFas treatment, mice were all alive when survived for the first 10 days after MI. Thus, when the survival was evaluated later than 10 days after MI, the survival of sFas-treated mice was significantly better than that of the LacZ-treated mice (P=0.0389; Figure 7).

The echocardiographic and hemodynamic evaluations of the surviving mice revealed that the beneficial effects of sFas gene delivery on post-MI cardiac function were preserved, even up to 10 weeks after MI (Figure 8). The necropsy study revealed that the greater MI wall thickness and smaller MI segmental length in the sFas-treated group was preserved (Figure 8). These findings indicate that the effect of sFas gene therapy persisted for many weeks, even after the exogenous sFas level had become undetectable.

Ineffectiveness of the sFas Gene Delivery During the Chronic Stage of MI

In further experiments, we checked whether inhibition of granulation tissue cell apoptosis is really responsible for the beneficial effects on post-MI heart failure. For this purpose, the sFas gene therapy was started at a more chronic stage of MI when granulation tissue has already disappeared; the sFas or LacZ gene (n=10 each) was delivered to mice with a 6-week-old MI that consisted not of granulation tissue but of scar tissue, and these mice were examined an additional 4 weeks later (10 weeks after MI). This time, we found no difference in functional and pathological parameters between the sFas-treated and LacZ-treated groups (Figure 8). These results clearly indicate that the preventive effect of the sFas gene therapy on heart failure is attributable to inhibition of granulation tissue cell apoptosis.

Discussion

In the present study, we suggested a significant role for Fas/Fas ligand interaction in the apoptosis of granulation tissue cells in myocardial infarct areas at the subacute stage of MI. Granulation tissue cells disappear naturally via apoptosis to eventually make a scar tissue.[14] The present study revealed that suppression of granulation tissue cell apoptosis by interfering with the Fas/Fas ligand interaction through sFas gene delivery resulted: anatomically, in attenuation of unfavorable remodeling of the LV; and functionally, in amelioration of cardiac dysfunction at the chronic stage of MI.

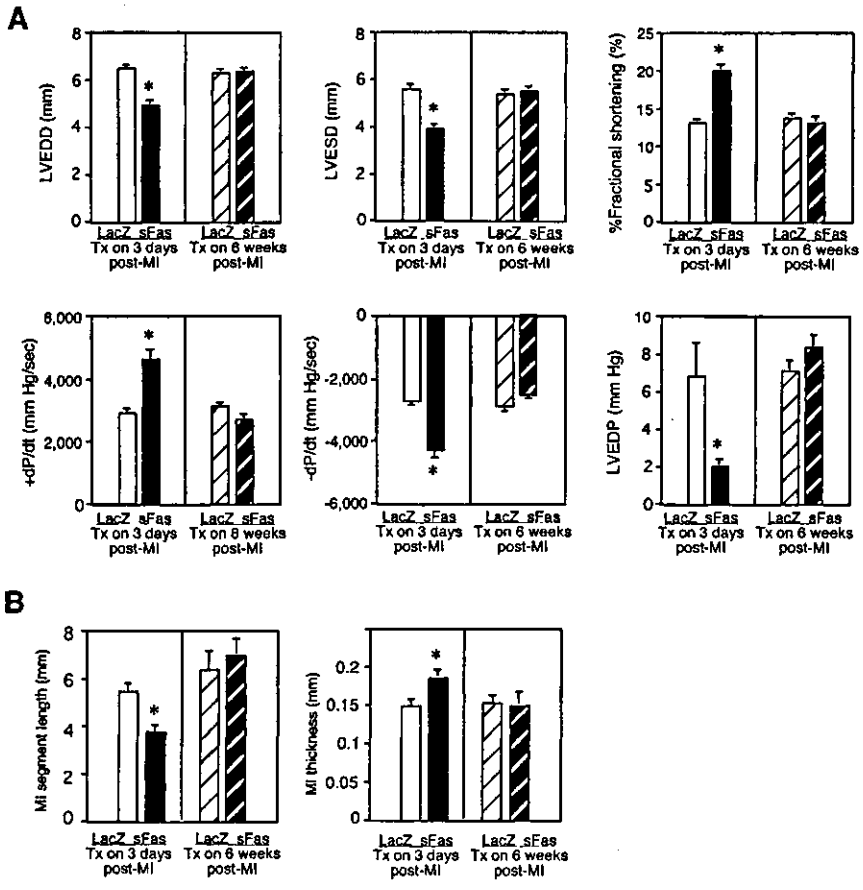

Figure 8. sFas gene delivery was effective even 10 weeks after MI, when it was applied at the subacute stage of MI (3 days after MI), whereas it was ineffective when applied at the chronic stage of MI (6 weeks after MI). Graphs show anatomical, hemodynamic, and pathological data for hearts at the chronic stage of MI (10 weeks after MI) obtained from echocardiography, cardiac catheterization, and necropsy study. *P<0.05 compared with the LacZ gene–delivered mice.

Post-MI survival during the chronic stage (later than the subacute stage) was also affected by the treatment. The results of the treatment were interesting, especially in terms of cardiac structure at the chronic stage: a thickened infarct wall developed containing abundant cellular components such as vessels and α-SMA–positive cells, part of which were found to be contractile phenotype smooth muscle cells under an electron microscope. The following are mechanistic considerations of the beneficial effects of the inhibition of granulation tissue cell apoptosis. First, the influence of infarct tissue geometry may be most important (ie, the shortening of the infarct segment length and increase in the infarct wall thickness). Contraction of the infarct tissue contributes to the suppression of ventricular dilatation. Because wall stress is proportional to the cavity diameter and inversely proportional to the wall thickness (Laplace's law),[26] and because wall stress and ventricular remodeling (dilatation) have a vicious relationship, accelerating each other, it is conceivable that such an alteration of infarct tissue geometry would bring a marked benefit of improving the hemodynamic state. Also, a smaller aneurysm has a lesser effect on cardiac function. Second, bundles of smooth muscle cells with a contractile phenotype in the infarct area, running in parallel with the surviving myocytes, might aid the global contractility of the LV. Third, the preservation of vessels might relieve ischemia in the surviving tissue. On the other hand, inhibition of cardiomyocyte apoptosis was not considered important because of the lack of TUNEL-positive cardiomyocytes during the subacute stage of MI, even in the LacZ-treated hearts. Compensatory hypertrophy of cardiomyocytes was independent of the beneficial effects because the cardiomyocytes were smaller in the sFas-treated than LacZ-treated hearts.

Although we showed the beneficial effect of the inhibition of granulation tissue apoptosis after MI, it should be cautioned that the benefit was evident in cases with large, transmural infarcts; the outcome would be unknown if the therapy were applied to cases with subendocardial infarction.

In the present study, we suggested that the apoptosis of each cell type of postinfarction granulation tissue is, at least in part, Fas dependent. However, macrophages continued to die, whereas vascular endothelial cells and myofibroblasts, having escaped a strong proapoptotic environment (granulation tissue as an inflammatory focus) by antiapoptotic treatment (sFas gene therapy), might continue to live until later. Speculatively, macrophages may have a higher sensitivity to apoptotic stimuli compared with the other preserved cells because inflammatory cells generally show very active proapoptotic interactions through death ligands and receptors.[16]

Fas was not immunohistochemically detected in cardiomyocytes under the present staining conditions. However, immunohistochemical negativity does not always deny the slight expression of an antigen because the sensitivity depends on the staining conditions. Several previous reports have shown immunohistochemically Fas expression in the cardiomyocytes of rats[27,28] and of humans.[29] Thus, it may be possible that our immunostaining method for Fas was less sensitive compared with those used in the previous studies. Notwithstanding, we detected Fas expression in the granulation tissue cells. This fact indicates that Fas expression in granulation tissue cells is definitely stronger than that in cardiomyocytes and suggests that the role of the Fas/Fas interaction in granulation tissue cells may be more significant than that in cardiomyocytes.

Postinfarct heart failure affects nearly half of all candidates for cardiac transplantation[30] and is one of the most serious clinical problems to be overcome in cardiovascular medicine. Recently, we reported that the inhibition of granulation tissue cell apoptosis by a pancaspase inhibitor after MI had beneficial effects on cardiac remodeling and dysfunction at the chronic stage of MI. The present study confirmed this therapeutic concept. However, because most of the apoptosis in a physiological setting is considered caspase dependent,[31] the systemic suppression of caspases may potentially have unfavorable effects on healthy organs. Actually, caspase 3-deficient homozygous mice undergo embryonic death.[32] On the basis of these facts, inhibition of the Fas/Fas ligand interaction may be a more specific way to apoptosis inhibition than inhibition of caspases. Our findings may warrant a therapeutic trial against postinfarction heart failure, which could be performed even during the subacute stage of MI in patients who have a large MI because the chance of reperfusion therapy during the acute stage has been lost. Thus, we expect the "inhibition of granulation tissue cell apoptosis" to become a novel therapeutic regimen that is prophylactic against chronic heart failure after large MI.

Acknowledgments

We thank Akiko Tsujimoto, Hatsue Ohshika, and the staff of Kyoto Women's University (Kaori Abe, Keiko Uodzu, Kazumi Ohara, Hitomi Takagaki, Machiko Mizutani, and Miyuki Morikawa) for technical assistance.

References

1. Pfeffer MA. Left ventricular remodeling after acute myocardial infarction. *Annu Rev Med.* 1995;46:455–466.
2. Reimer KA, Vander Heide RS, Richard VJ. Reperfusion in acute myocardial infarction: effect of timing and modulating factors in experimental models. *Am J Cardiol.* 1993;72:13G–21G.
3. McKay RG, Pfeffer MA, Pasternak RC, Markis JE, Come PC, Nakao S, Alderman JD, Ferguson JJ, Safian RD, Grossman W. Left ventricular remodeling after myocardial infarction: a corollary to infarct expansion. *Circulation.* 1986;74:693–702.
4. Weisman HF, Bush DE, Mannisi JA, Weisfeldt ML, Healy B. Cellular mechanisms of myocardial infarct expansion. *Circulation.* 1988;78:186–201.
5. Cheng W, Kajstura J, Nitahara JA, Li B, Reiss K, Liu Y, Clark WA, Krajewski S, Reed JC, Olivetti G, Anversa P. Programmed myocyte cell death affects the viable myocardium after infarction in rats. *Exp Cell Res.* 1996;226:316–327.
6. Shan K, Kurrelmeyer K, Seta Y, Wang F, Dibbs Z, Deswal A, Lee-Jackson D, Mann DL. The role of cytokines in disease progression in heart failure. *Curr Opin Cardiol.* 1997;12:218–223.
7. Olivetti G, Abbi R, Quaini F, Kajstura J, Cheng W, Nitahara JA, Quaini E, Di Loreto C, Beltrami CA, Krajewski S, Reed JC, Anversa P. Apoptosis in the failing human heart. *N Engl J Med.* 1997;336:1131–1141.
8. Narula J, Kolodgie FD, Virmani R. Apoptosis and cardiomyopathy. *Curr Opin Cardiol.* 2000;15:183–188.
9. Gill C, Mestril R, Samali A. Losing heart: the role of apoptosis in heart disease—a novel therapeutic target? *FASEB J.* 2002;16:135–146.
10. Elsässer A, Suzuki K, Schaper J. Unresolved issues regarding the role of apoptosis in the pathogenesis of ischemic injury and heart failure. *J Mol Cell Cardiol.* 2000;32:711–724.
11. Kang PM, Izumo S. Apoptosis and heart failure: a critical review of the literature. *Circ Res.* 2000;86:1107–1113.
12. Hayakawa K, Takemura G, Koda M, Kawase Y, Maruyama R, Li Y, Minatoguchi S, Fujiwara T, Fujiwara H. Sensitivity to apoptosis signal,

clearance rate, and ultrastructure of Fas ligand-induced apoptosis in in vivo adult cardiac cells. *Circulation.* 2002;105:3039–3045.
13. Kostin S, Pool L, Elsässer A, Hein S, Drexler HC, Arnon E, Hayakawa Y, Zimmermann R, Bauer E, Klovekorn WP, Schaper J. Myocytes die by multiple mechanisms in failing human hearts. *Circ Res.* 2003;92: 715–724.
14. Takemura G, Ohno M, Hayakawa Y, Misao J, Kanoh M, Ohno A, Uno Y, Minatoguchi S, Fujiwara T, Fujiwara H. Role of apoptosis in the disappearance of infiltrated and proliferated interstitial cells after myocardial infarction. *Circ Res.* 1998;82:1130–1138.
15. Hayakawa K, Takemura G, Kanoh M, Li Y, Koda M, Kawase Y, Maruyama R, Okada H, Minatoguchi S, Fujiwara T, Fujiwara H. Inhibition of granulation tissue cell apoptosis during the subacute stage of myocardial infarction improves cardiac remodeling and dysfunction at the chronic stage. *Circulation.* 2003;108:104–109.
16. Nagata S. Apoptosis by death factor. *Cell.* 1997;88:355–365.
17. Suda T, Hashimoto H, Tanaka M, Ochi T, Nagata S. Membrane Fas ligand kills human peripheral blood T lymphocytes, and soluble Fas ligand blocks the killing. *J Exp Med.* 1997;186:2045–2050.
18. Li Y, Takemura G, Kosai K, Yuge K, Nagano S, Esaki M, Goto K, Takahashi T, Hayakawa K, Koda M, Kawase Y, Maruyama R, Okada H, Minatoguchi S, Mizuguchi H, Fujiwara T, Fujiwara H. Postinfarction treatment with adenoviral vector expressing hepatocyte growth factor relieves chronic left ventricular remodeling and dysfunction in mice. *Circulation.* 2003;107:2499–2506.
19. Mizuguchi H, Kay AM. A simple method for constructing E1- and E1/E4-deleted recombinant adenoviral vectors. *Hum Gene Ther.* 1999; 10:2013–2017.
20. Suda T, Nagata S. Purification and characterization of the Fas-ligand that induces apoptosis. *J Exp Med.* 1994;179:873–879.
21. Chen SH, Chen XH, Wang Y, Kosai K, Finegold MJ, Rich SS, Woo SL. Combination gene therapy for liver metastasis of colon carcinoma in vivo. *Proc Natl Acad Sci U S A.* 1995;92:2577–2581.
22. Desmouliere A, Redard M, Darby I, Gabbiani G. Apoptosis mediates the decrease in cellularity during the transition between granulation tissue and scar. *Am J Pathol.* 1995;146:56–66.
23. Watanabe-Fukunaga R, Brannan CI, Copeland NG, Jenkins NA, Nagata S. Lymphoproliferation disorder in mice explained by defects in Fas antigen that mediates apoptosis. *Nature.* 1992;356:314–317.
24. Takahashi T, Tanaka M, Brannan CI, Jenkins NA, Copeland NG, Suda T, Nagata S. Generalized lymphoproliferative disease in mice, caused by a point mutation in the Fas ligand. *Cell.* 1994;76:969–976.
25. Nishigaki K, Minatoguchi S, Seishima M, Asano K, Noda T, Yasuda N, Sano H, Kumada H, Takemura M, Noma A, Tanaka T, Watanabe S, Fujiwara H. Plasma Fas ligand, an inducer of apoptosis, and plasma soluble Fas, an inhibitor of apoptosis, in patients with chronic congestive heart failure. *J Am Coll Cardiol.* 1997;29:1214–1220.
26. Yin FC. Ventricular wall stress. *Circ Res.* 1981;49:829–842.
27. Kajstura J, Cheng W, Reiss K, Clark WA, Sonnenblick EH, Krajewski S, Reed JC, Olivetti G, Anversa P. Apoptotic and necrotic myocyte cell deaths are independent contributing variables of infarct size in rats. *Lab Invest.* 1996;74:86–107.
28. Wollert KC, Heineke J, Westermann J, Ludde M, Fiedler B, Zierhut W, Laurent D, Bauer MK, Schulze-Osthoff K, Drexler H. The cardiac Fas (APO-1/CD95) Receptor/Fas ligand system: relation to diastolic wall stress in volume-overload hypertrophy in vivo and activation of the transcription factor AP-1 in cardiac myocytes. *Circulation.* 2000;101: 1172–1178.
29. Filippatos G, Leche C, Sunga R, Tsoukas A, Anthopoulos P, Joshi I, Bifero A, Pick R, Uhal BD. Expression of FAS adjacent to fibrotic foci in the failing human heart is not associated with increased apoptosis. *Am J Physiol.* 1999;277:H445–H451.
30. Hosenpud JD, Bennett LE, Keck BM, Boucek MM, Novick RJ. The registry of the International Society for Heart and Lung Transplantation: seventeenth official report-2000. *J Heart Lung Transplant.* 2000;19: 909–931.
31. Thornberry NA, Lazebnik Y. Caspases: enemies within. *Science.* 1998; 281:1312–1316.
32. Kuida K, Zheng TS, Na S, Kuan C, Yang D, Karasuyama H, Rakic P, Flavell RA. Decreased apoptosis in the brain and premature lethality in CPP32-deficient mice. *Nature.* 1996;384:368–372.